

PAPER • OPEN ACCESS

Dielectric response of electron–hole systems. Nondegenerate case and quantum corrections

To cite this article: D Semkat *et al* 2021 *J. Phys.: Condens. Matter* **33** 475501

View the [article online](#) for updates and enhancements.

You may also like

- [The effect of energy-dependent electron scattering on thermoelectric transport in novel topological semimetal CoSi](#)
D A Pshenay-Severin, Y V Ivanov and A T Burkov
- [Analysis of current crowding in thin film contacts from exact field solution](#)
Peng Zhang, Y Y Lau and R M Gilgenbach
- [Electrochemical phase diagrams of Ni from *ab initio* simulations: role of exchange interactions on accuracy](#)
Liang-Feng Huang and James M Rondinelli

Dielectric response of electron–hole systems. Nondegenerate case and quantum corrections

D Semkat¹ , H Stolz² , W-D Kraeft² and H Fehske¹

¹ Institut für Physik, Ernst-Moritz-Arndt-Universität Greifswald, Felix-Hausdorff-Str. 6, 17489 Greifswald, Germany

² Institut für Physik, Universität Rostock, Albert-Einstein-Str. 23-24, 18059 Rostock, Germany

E-mail: dirk.semkat@uni-greifswald.de

Received 22 April 2021, revised 12 August 2021

Accepted for publication 24 August 2021

Published 8 September 2021



Abstract

Analytical results for the dielectric function in RPA are derived for three-, two-, and one-dimensional semiconductors in the weakly-degenerate limit. Based on this limit, quantum corrections are derived. Further attention is devoted to systems with linear carrier dispersion and the resulting Dirac-cone physics.

Keywords: dielectric response, electron–hole plasma, quasi-two-dimensional systems, Dirac-cone physics, quantum corrections

(Some figures may appear in colour only in the online journal)

1. Introduction

The response of a medium to external electromagnetic fields is determined by its dielectric function [1]. The description of various phenomena is closely connected with this quantity, e.g. the buildup of screening or the behavior of bound states of electrons and holes in a semiconductor (excitons) surrounded by a plasma of free carriers [2, 3]. While in earlier times the main interest was focused on higher densities (see, e.g., [4]), with the observation of Rydberg excitons in cuprous oxide (Cu₂O) [5, 6] the behavior in a very low density plasma has become important, as Rydberg states due to their large Bohr radius (up to 1 μm for $n = 30$ [7]), are extremely sensitive to such a low density plasma. In a recent study we have shown that the Mott effect, i.e., the vanishing of a bound state at a certain plasma density, occurs for quantum number $n = 25$ already at a density of 10^8 cm^{-3} . Most important, however, is that, despite the low density, the commonly used Debye approximation [2]

gives completely wrong results [8, 9]. Crucial in these calculations was the use of an exact expression for the dielectric function. To extend these studies to two-dimensional systems such as transition metal dichalcogenide monolayers [10] and even to one-dimensional systems, one has to know the exact dielectric function also for lower dimensionality.

A further example are the collective oscillation modes of this plasma (plasmons), the complex energies of which are given by the zeros of the complex dielectric function. Knowledge on this function is, therefore, essential for the understanding of various optical and transport properties of semiconductors.

In the current paper we derive and discuss analytical results for the dielectric function in *random phase approximation* (RPA). Section 3 is devoted to the case of bulk systems. Afterward in section 4 we discuss lower-dimensional systems. Finally, in section 5 we show an extension of the results to moderate degeneracy, i.e., derive quantum corrections to the nondegenerate limit.

Some derivations are presented in the appendices, e.g., the effective Coulomb potential for quasi-two-dimensional systems (appendix A) and the dielectric function for the one-dimensional case (B). The quite distinct case of linear quasiparticle dispersion, which occurs in graphene [11] and

* Author to whom any correspondence should be addressed.



Original content from this work may be used under the terms of the [Creative Commons Attribution 4.0 licence](https://creativecommons.org/licenses/by/4.0/). Any further distribution of this work must maintain attribution to the author(s) and the title of the work, journal citation and DOI.

topological quantum matter [12] with Dirac-cone functionality is analyzed on the same footing in appendix C.

2. Polarization function

The dielectric function of an electron–hole plasma in a d -dimensional semiconductor is connected via

$$\epsilon(k, \omega) = 1 - \sum_{a=e,h} V_{aa}(k) \Pi_{aa}(k, \omega) \quad (1)$$

with the polarization function Π_{aa} of electrons and holes ($a = e, h$), respectively [2]. V_{aa} is the dimension-dependent interaction potential between carriers of species a . In RPA, the polarization function is given by the well-known Lindhard expression [2]

$$\Pi_{aa}(k, \omega) = (2s_a + 1) \int \frac{d^d q}{(2\pi)^d} \times \frac{f_a\left(\frac{\mathbf{k}}{2} - \mathbf{q}\right) - f_a\left(\frac{\mathbf{k}}{2} + \mathbf{q}\right)}{E_a\left(\frac{\mathbf{k}}{2} - \mathbf{q}\right) - E_a\left(\frac{\mathbf{k}}{2} + \mathbf{q}\right) + \hbar\omega + i\epsilon}. \quad (2)$$

Here f_a is the distribution function of species a which is, in the nondegenerate case, given by the Boltzmann distribution

$$f_a(k) = \frac{n_a \Lambda_a^d}{2s_a + 1} \exp\left(-\frac{\hbar^2 k^2}{2m_a k_B T_a}\right) \quad (3)$$

with temperature T_a and density n_a of species a . Λ_a is the thermal de Broglie wavelength,

$$\Lambda_a = \left(\frac{2\pi\hbar^2}{m_a k_B T_a}\right)^{1/2} \quad (4)$$

and $2s_a + 1$ is the spin degeneracy factor which is for electrons and holes $2s_a + 1 = 2$. The quasiparticle energies E_a are approximated by free particle energies [13] which read, in the usual approximation of parabolic bands,

$$E_a(k) = \frac{\hbar^2 k^2}{2m_a} + \text{Re}\Sigma_a(\mathbf{k}, \omega) \Big|_{\omega=E_a(\mathbf{k})/\hbar} \approx \frac{\hbar^2 k^2}{2m_a}. \quad (5)$$

It is well known and frequently cited that the integral in (2) can be evaluated in the nondegenerate case (for $d = 3$) analytically [4, 14, 15]. Reference [16] is regarded as the key source, however, the explicit derivation cannot be found in that work. Moreover, in the mentioned papers, the three-dimensional (3d) case is (implicitly) assumed. We will, therefore, rederive the ‘classical’ result in 3d and consider afterward the 2d and 1d cases.

3. Bulk semiconductor

In the case of a bulk semiconductor, the interaction potential between carriers of species a V_{aa} ($a = e, h$) is given by the three-dimensional Coulomb potential V_{aa}^C ,

$$V_{aa}^C(k) = \frac{e_a e_a}{\epsilon_0 \epsilon_b} \frac{1}{k^2} = \frac{e^2}{\epsilon_0 \epsilon_b} \frac{1}{k^2} \quad (6)$$

with ϵ_b being the background dielectric constant. The integral in (2) can be written in spherical coordinates (q, ϑ, φ) . We lay the z -axis of the \mathbf{q} -integration into \mathbf{k} . The difference in the numerator of (2) then becomes

$$\begin{aligned} f_a\left(\frac{\mathbf{k}}{2} - \mathbf{q}\right) - f_a\left(\frac{\mathbf{k}}{2} + \mathbf{q}\right) &= \frac{n_a \Lambda_a^3}{2} \exp\left[-\frac{\hbar^2}{2m_a k_B T_a} \left(\frac{k^2}{4} + q^2\right)\right] \\ &\times \left[\exp\left(\frac{\hbar^2}{2m_a k_B T_a} kq \cos \vartheta\right) - \exp\left(-\frac{\hbar^2}{2m_a k_B T_a} kq \cos \vartheta\right) \right]. \end{aligned} \quad (7)$$

Using (5) the energy difference in the denominator of (2) is

$$\begin{aligned} E_a\left(\frac{\mathbf{k}}{2} - \mathbf{q}\right) - E_a\left(\frac{\mathbf{k}}{2} + \mathbf{q}\right) &= \frac{\hbar^2}{2m_a} \left[\left(\frac{\mathbf{k}}{2} - \mathbf{q}\right)^2 - \left(\frac{\mathbf{k}}{2} + \mathbf{q}\right)^2 \right] \\ &= -\frac{\hbar^2}{m_a} kq \cos \vartheta. \end{aligned} \quad (8)$$

Inserting the differences (7) and (8) into (2), substituting in the usual manner $\cos \vartheta = t$ and performing the trivial φ -integration, the polarization function reads

$$\begin{aligned} \Pi_{aa}^{(3d)}(k, \omega) &= \frac{1}{(2\pi)^2} n_a \Lambda_a^3 \exp\left(-\frac{\hbar^2 k^2}{8m_a k_B T_a}\right) \\ &\times \int_0^\infty dq q^2 \exp\left(-\frac{\hbar^2 q^2}{2m_a k_B T_a}\right) \\ &\times \int_{-1}^1 dt \frac{\exp\left(\frac{\hbar^2}{2m_a k_B T_a} kqt\right) - \exp\left(-\frac{\hbar^2}{2m_a k_B T_a} kqt\right)}{\hbar\omega - \frac{\hbar^2}{m_a} kqt + i\epsilon}. \end{aligned} \quad (9)$$

For the following calculations, we introduce the abbreviations $\beta = 1/(k_B T_a)$, $a = \hbar^2/(2m_a)$, and $w = \hbar\omega$ and substitute $akq = x$. The double integral to be evaluated reads now

$$I = \frac{1}{a^3 k^3} \int_0^\infty dx x^2 \exp\left(-\frac{\beta}{ak^2} x^2\right) \int_{-1}^1 dt \frac{e^{\beta xt} - e^{-\beta xt}}{w - 2xt + i\epsilon}. \quad (10)$$

We separate real and imaginary parts by expanding with the complex conjugate of the denominator,

$$\begin{aligned} I &= \frac{1}{a^3 k^3} \int_0^\infty dx x^2 \exp\left(-\frac{\beta}{ak^2} x^2\right) \int_{-1}^1 dt (e^{\beta xt} - e^{-\beta xt}) \\ &\times \left\{ \frac{w - 2xt}{(w - 2xt)^2 + \epsilon^2} - \frac{i\epsilon}{(w - 2xt)^2 + \epsilon^2} \right\} \\ &= I_1 + I_2. \end{aligned} \quad (11)$$

The imaginary part I_2 can be evaluated easily. We perform in this term the limit $\epsilon \rightarrow 0$, obtaining

$$I_2 = -\frac{i\pi}{a^3k^3} \int_0^\infty dx x^2 \exp\left(-\frac{\beta}{ak^2}x^2\right) \times \int_{-1}^1 dt (e^{\beta xt} - e^{-\beta xt}) \delta(w - 2xt). \quad (12)$$

Performing subsequently t - and x -integration yields

$$I_2 = -\frac{i\pi}{4\beta a^2k} \left(e^{\beta w/2} - e^{-\beta w/2}\right) \exp\left(-\frac{\beta w^2}{4ak^2}\right). \quad (13)$$

In its present form, the real part I_1 cannot be solved straightforwardly. Therefore, we introduce an auxiliary integral by making use of

$$\frac{1}{y} = \int_0^\infty ds e^{-ys} \quad \text{for } y > 0. \quad (14)$$

After rearranging the exponentials, changing the order of integrations, and substituting $4s = z$, integral I_1 then reads

$$I_1 = \frac{1}{4a^3k^3} \int_0^\infty dz \exp\left[-\frac{1}{4}(w^2 + \epsilon^2)z\right] \times \int_0^\infty dx x^2 \exp\left(-\frac{\beta}{ak^2}x^2\right) \int_{-1}^1 dt \exp(-x^2zt^2) \times \{\exp[(wz + \beta)xt] - \exp[(wz - \beta)xt]\} (w - 2xt). \quad (15)$$

The t -, x -, and z -integrals can now be performed subsequently yielding (note that the limit $\epsilon \rightarrow 0$ can be done trivially)

$$I_1 = -\frac{\sqrt{\pi}}{2\beta a^2k} \exp\left(\frac{\beta ak^2}{4}\right) \left\{ F\left[\frac{\sqrt{\beta}}{2\sqrt{ak}}(w + ak^2)\right] - F\left[\frac{\sqrt{\beta}}{2\sqrt{ak}}(w - ak^2)\right] \right\}, \quad (16)$$

where F denotes Dawson's integral which is closely connected with the confluent hypergeometric function ${}_1F_1$ (also referred to as Kummer function) and with the Faddeeva function (or Kramp function) w [17],

$$F(x) = \int_0^x dt \exp(t^2 - x^2) = x {}_1F_1\left(1, \frac{3}{2}; -x^2\right) = \frac{\sqrt{\pi}}{2} \text{Im } w(x). \quad (17)$$

The latter function is in turn connected to the complementary complex error function,

$$w(x) = \exp(-x^2) \text{erfc}(-ix), \quad (18)$$

i.e., its real part is given by $\text{Re } w(x) = \exp(-x^2)$ ($x \in \mathbb{R}$). Therefore, we can combine (16) and (13),

$$e^{-\frac{\beta ak^2}{4}}(I_1 + I_2) = -\frac{\pi}{4\beta a^2k} \left\{ \frac{2}{\sqrt{\pi}} \left\{ F\left[\frac{\sqrt{\beta}}{2\sqrt{ak}}(w + ak^2)\right] - F\left[\frac{\sqrt{\beta}}{2\sqrt{ak}}(w - ak^2)\right] \right\} + i \left\{ \exp\left[-\frac{\beta}{4ak^2}(w - ak^2)^2\right] - \exp\left[-\frac{\beta}{4ak^2}(w + ak^2)^2\right] \right\} \right\} = \frac{i\pi}{4\beta a^2k} \left\{ w \left[\frac{\sqrt{\beta}}{2\sqrt{ak}}(w + ak^2)\right] - w \left[\frac{\sqrt{\beta}}{2\sqrt{ak}}(w - ak^2)\right] \right\}. \quad (19)$$

Inserting the result (19) into the polarization function (9) we get for the latter quantity

$$\Pi_{aa}^{(3d)}(k, \omega) = \frac{1}{(2\pi)^2} n_a \Lambda_a^3 \frac{i\pi}{4\beta a^2k} \left\{ w \left[\frac{\sqrt{\beta}}{2\sqrt{ak}}(w + ak^2)\right] - w \left[\frac{\sqrt{\beta}}{2\sqrt{ak}}(w - ak^2)\right] \right\} = i \frac{\sqrt{\pi}}{2} n_a \sqrt{\frac{2m_a}{\hbar^2 k^2}} \frac{1}{\sqrt{k_B T_a}} \times \left\{ w \left[\frac{1}{2\sqrt{k_B T_a}} \sqrt{\frac{2m_a}{\hbar^2 k^2}} \left(\hbar\omega + \frac{\hbar^2 k^2}{2m_a}\right)\right] - w \left[\frac{1}{2\sqrt{k_B T_a}} \sqrt{\frac{2m_a}{\hbar^2 k^2}} \left(\hbar\omega - \frac{\hbar^2 k^2}{2m_a}\right)\right] \right\}. \quad (20)$$

We finally use the dimensionless quantities

$$x = \frac{1}{2} \frac{\omega/\omega_e}{k/\kappa}, \quad y = \left(\frac{\hbar^2 k^2}{8m_e k_B T_a}\right)^{1/2}, \quad s = \left(\frac{m_h}{m_e}\right)^{1/2}, \quad \kappa = \left(\frac{2n_e e^2}{\epsilon_0 \epsilon_b k_B T_a}\right)^{1/2}, \quad \omega_e = \left(\frac{n_e e^2}{\epsilon_0 \epsilon_b m_e}\right)^{1/2}, \quad (21)$$

where κ and ω_e are inverse screening length and plasma frequency of the electrons, respectively. Summing up Π_{ee} and Π_{hh} , one arrives at

$$\varepsilon(k, \omega) = 1 - i \frac{\sqrt{\pi}}{4} \frac{\kappa^2}{k^2} \left[\frac{w(x+y) - w(x-y)}{2y} + \frac{w(sx+y/s) - w(sx-y/s)}{2y/s} \right]. \quad (22)$$

For the first time, this result has been derived in [16]. In the form of (22), it agrees with (19) in [15].

Figure 1 shows real and imaginary parts of $\varepsilon(q, \omega) - 1$. We consider electrons and holes in bulk Cu_2O with the parameters: electron mass $m_e = 0.985m_0$, hole mass $m_h = 0.575m_0$, and dielectric constant $\epsilon_b = 7.507$. Since figure 1 serves here

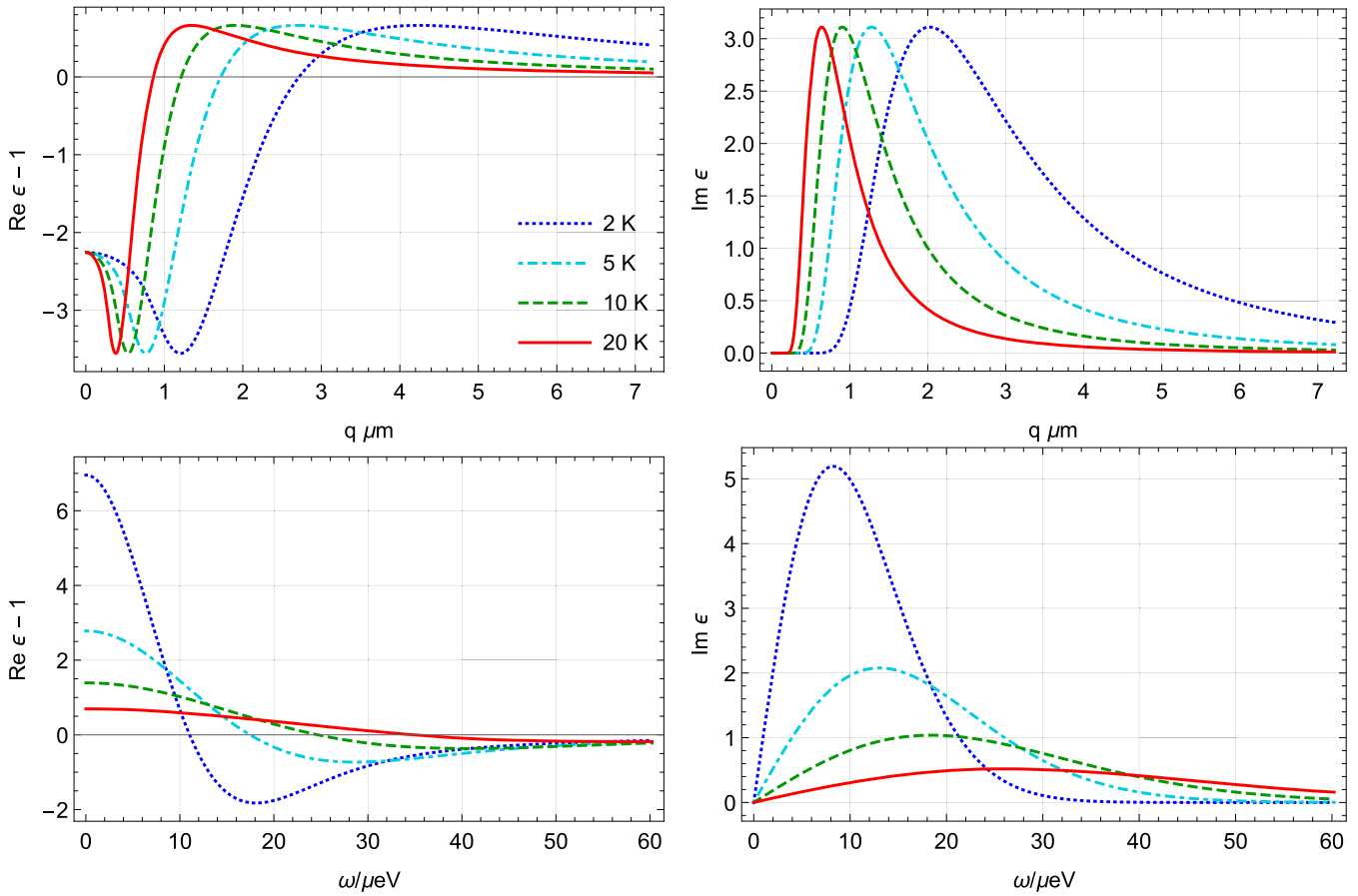


Figure 1. Real (left panels) and imaginary parts (right panels) of the dielectric function vs wave number q at a frequency of $\hbar\omega = 15 \mu\text{eV}$ (upper row) and vs frequency at a wave number of $q = 2 \mu\text{m}^{-1}$ (lower row) for electrons and holes in bulk cuprous oxide, each for a carrier density of $n = 10^{12} \text{ cm}^{-3}$ and several temperatures.

mainly for illustration of the considered quantity, we only briefly mention the contained physical information, i.e., the dispersion of collective plasma modes (plasmons) given by the zeros of $\text{Re } \epsilon$ and their damping connected with $\text{Im } \epsilon$.

4. Two-dimensional semiconductor structures

In two dimensions, the Coulomb potential is proportional to $\log r$ instead of $1/r$ as in 3d (corresponding to $1/k$ instead of $1/k^2$). Semiconductor structures like GaAs/AlGaAs quantum wells or TMDC monolayers are quasi-two-dimensional, i.e., the layer widths are small compared to their in-plane extension.

One possibility to handle this quasi-two-dimensionality is to use for the interaction potential V_{aa} the Rytova–Keldysh potential [18, 19]. Usually given in its quite complicated form in configuration space, it reads in momentum space simply [20]

$$V_{aa}^{\text{RK}}(q) = \frac{e^2}{2\epsilon_0\epsilon_{\text{sub}}A} \frac{1}{q(1+r_0q)}, \quad (23)$$

where ϵ_{sub} is the mean dielectric constant of the substrates and r_0 the screening length, $r_0 = d_0\epsilon_{\perp}/\epsilon_{\text{sub}}$ with ϵ_{\perp} being the dielectric constant of the monolayer and d_0 its thickness.

Depending on the latter parameter, the potential (23) interpolates between the limiting cases of bulk material ($r_0q \gg 1$) and true 2d system ($r_0q \rightarrow 0$).

Another way is to account for the confinement in the third dimension by the respective eigenfunctions of the carriers in the quantum well [21, 22],

$$V_{ab}(q) = \frac{e_a e_b}{2\epsilon_0\epsilon_{b,w}q} \int_{-\infty}^{\infty} dz \int_{-\infty}^{\infty} dz' |\Phi_a(z)|^2 |\Phi_b(z')|^2 \times \exp(-q|z-z'|), \quad (24)$$

where $\Phi_{a/b}$ are the wave functions of the motion in confinement- (z)-direction, $\epsilon_{b,w}$ is the background dielectric constant in the well, and $e_{e/h} = \mp e$. An analytical expression for this effective quasi-two-dimensional potential is derived in appendix A.

We consider a 2d system again with parabolic carrier dispersion. In that case, polar coordinates (q, φ) seem to be convenient for the integral in (2), however, Cartesian coordinates (q_x, q_y) turn out to be the appropriate choice. The polarization function then reads

$$\Pi_{aa}^{(2d)}(k, \omega) = \frac{1}{2\pi} n_a \Lambda_a^2 \exp\left(-\frac{\hbar^2 k^2}{8m_a k_B T_a}\right) I \quad (25)$$

with

$$I = \frac{1}{a^2 k_x k_y} \int_{-\infty}^{\infty} dx \int_{-\infty}^{\infty} dy \exp[-(ux^2 + vy^2)] \times [e^{\beta(x+y)} - e^{-\beta(x+y)}] \times \left\{ \frac{w - 2(x+y)}{[w - 2(x+y)]^2 + \epsilon^2} - \frac{i\epsilon}{[w - 2(x+y)]^2 + \epsilon^2} \right\} = I_1 + I_2, \quad (26)$$

where we have introduced the abbreviations $x = ak_x q_x$, $y = ak_y q_y$, $u = \beta/(ak_x^2)$, and $v = \beta/(ak_y^2)$.

Like in the previous section, we look at first at the second (imaginary) contribution I_2 . Performing the limit $\epsilon \rightarrow 0$ and substituting $s = 2(x+y)$ (i.e. $(x, y) \rightarrow (x, s)$) leads to

$$I_2 = -\frac{i\pi}{2a^2 k_x k_y} \int_{-\infty}^{\infty} dx \int_{-\infty}^{\infty} ds \exp \left\{ - \left[ux^2 + v \left(\frac{s}{2} - x \right)^2 \right] \right\} \times \left[\exp \left(\frac{\beta s}{2} \right) - \exp \left(-\frac{\beta s}{2} \right) \right] \delta(w - s) \quad (27)$$

which yields straightforwardly

$$I_2 = -\frac{i\sqrt{\pi^3}}{2\sqrt{\beta a^3 k}} \left[\exp \left(\frac{\beta w}{2} \right) - \exp \left(-\frac{\beta w}{2} \right) \right] \exp \left(-\frac{\beta w^2}{4ak^2} \right). \quad (28)$$

In the first (real) contribution to I (26) we apply again the integration trick (14),

$$I_1 = \frac{1}{a^2 k_x k_y} \int_0^{\infty} dz \exp[-(w^2 + \epsilon^2)z] \int_{-\infty}^{\infty} dx \times \int_{-\infty}^{\infty} dy \exp[-(u + 4z)x^2] \times \exp[-(v + 4z)y^2] \exp(-8xyz)[w - 2(x+y)] \times \{ \exp[(\beta + 4wz)(x+y)] - \exp[-(\beta - 4wz)(x+y)] \}. \quad (29)$$

Now the integrations can be performed subsequently leading to the result

$$I_1 = \frac{\pi}{\sqrt{\beta a^3 k}} \exp \left(\frac{\beta ak^2}{4} \right) \left\{ F \left[\frac{\sqrt{\beta}}{2\sqrt{ak}} (w - ak^2) \right] - F \left[\frac{\sqrt{\beta}}{2\sqrt{ak}} (w + ak^2) \right] \right\},$$

where F again denotes Dawson's integral.

Analogously to (19), we can sum up the real and imaginary parts and express them in terms of the Faddeeva function w so that we finally get for the polarization function

$$\Pi_{aa}^{(2d)}(k, \omega) = \frac{1}{(2\pi)^2} n_a \Lambda_a^2 \frac{i\sqrt{\pi^3}}{2\sqrt{\beta a^3 k}} \times \left\{ w \left[\frac{\sqrt{\beta}}{2\sqrt{ak}} (w + ak^2) \right] - w \left[\frac{\sqrt{\beta}}{2\sqrt{ak}} (w - ak^2) \right] \right\}$$

$$= i \frac{\sqrt{\pi}}{2} n_a \sqrt{\frac{2m_a}{\hbar^2 k^2}} \frac{1}{\sqrt{k_B T_a}} \times \left\{ w \left[\frac{1}{2\sqrt{k_B T_a}} \sqrt{\frac{2m_a}{\hbar^2 k^2}} \left(\hbar\omega + \frac{\hbar^2 k^2}{2m_a} \right) \right] - w \left[\frac{1}{2\sqrt{k_B T_a}} \sqrt{\frac{2m_a}{\hbar^2 k^2}} \left(\hbar\omega - \frac{\hbar^2 k^2}{2m_a} \right) \right] \right\}. \quad (30)$$

Comparing the 3d and 2d results (20) and (30), we see that both cases have the same form, but note the different character and dimension of n_a —bulk density vs area density, i.e., $\Pi_{aa}^{(2d)}(k, \omega) = \Pi_{aa}^{(3d)}(k, \omega)$.

A very similar, straightforward calculation in the 1d case yields the corresponding result (see appendix B), i.e., the functional form of the RPA polarization function of the electron–hole plasma in the nondegenerate limit is independent on the dimensionality of the system.

In all cases considered above we assumed the usual parabolic approximation for valence and conduction bands leading to free-particle-like dispersions of electrons and holes. There are, however, quasi-two-dimensional systems (the probably most prominent being graphene) where the band structure gives rise to linear carrier dispersions ($E(\mathbf{k}) = \gamma k$) and exhibits so-called Dirac cones near the charge neutrality point. The polarization function in such systems is usually considered in the highly degenerate limiting case [23–26], however, an analytical expression for a model system with linear dispersion in the case of weak degeneracy can be obtained, too, see appendix C.

5. Extension to moderate degeneracy

So far, the analysis relied on the assumption of very weak degeneracy of the carriers which allows to assume Boltzmann distributions (3). Now we look more closely at the distribution function. It reads for arbitrary degeneracy (Fermi distribution)

$$f_a(k) = \frac{1}{\exp \left(\frac{\hbar^2 k^2}{2m_a k_B T_a} - \mu_a \right) + 1}, \quad (31)$$

where μ_a is the chemical potential of species a . Introducing the fugacity $z = e^{\beta\mu}$ and abbreviating the Boltzmann factor $b = \exp \left(-\frac{\hbar^2 k^2}{2m_a k_B T_a} \right)$ one can write

$$f_a(k) = \frac{1}{z^{-1}b^{-1} + 1} = \frac{zb}{1 + zb} = zb(1 - zb + z^2b^2 - z^3b^3 + \dots), \quad (32)$$

where the last equality holds for $z < 1$, i.e., for weak to moderate degeneracy. The Boltzmann factor to an arbitrary power j reads

$$b^j = \exp \left(-j \frac{\hbar^2 k^2}{2m_a k_B T_a} \right) = \exp \left(-\frac{\hbar^2 k^2}{2m_a k_B (T_a/j)} \right), \quad (33)$$

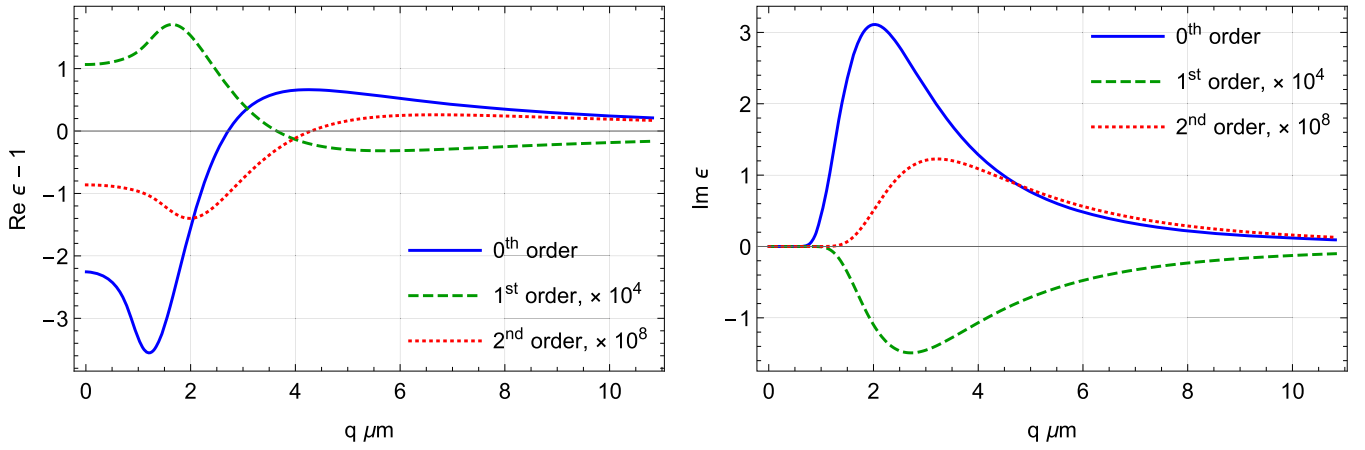


Figure 2. Quantum correction terms of first and second order to the real (left panel) and imaginary (right panel) parts of the dielectric function of electrons and holes in bulk Cu₂O compared to the nondegenerate case vs wave number q at frequency $\hbar\omega = 15 \mu\text{eV}$ for temperature $T = 2 \text{ K}$ and carrier density $n = 10^{12} \text{ cm}^{-3}$. Note the magnification factors of the first and second order terms.

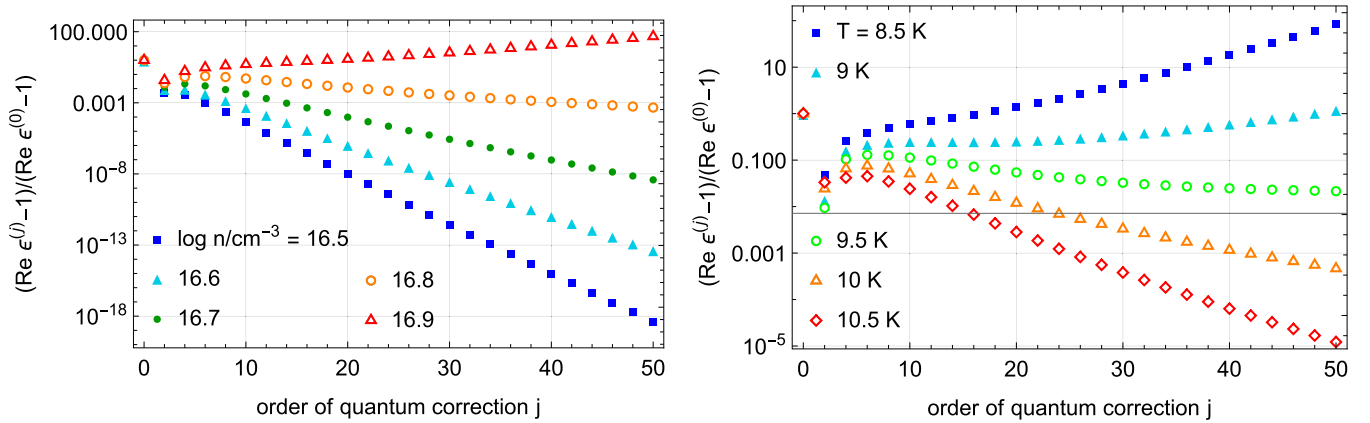


Figure 3. Quantum correction term of j th order to the real part of the dielectric function normalized to the nondegenerate term vs order j for a temperature of $T = 10 \text{ K}$ and several carrier densities (left panel) and for $\log n/\text{cm}^{-3} = 16.5$ and several temperatures (right panel).

i.e., it corresponds to a Boltzmann factor with an effective temperature T/j . We get

$$f_a(k) = z \exp\left(-\frac{\hbar^2 k^2}{2m_a k_B T_a}\right) \sum_{j=0}^{\infty} (-1)^j z^j \times \exp\left(-\frac{\hbar^2 k^2}{2m_a k_B (T_a/j)}\right) = \sum_{j=1}^{\infty} (-1)^{j-1} z^j \exp\left(-\frac{\hbar^2 k^2}{2m_a k_B (T_a/j)}\right). \quad (34)$$

The difference of distribution functions occurring in Π (2) can be calculated in every order of the expansion (34) analogously to (7) (or in the Cartesian analogue leading to (25) and (26), respectively). Therefore, the calculation in each order is the same as presented in the previous sections. The result is a series for Π ,

$$\Pi_{aa}^{\text{qc}}(k, \omega; T_a) = \frac{2}{n_a \Lambda_a^d} \sum_{j=1}^{\infty} \frac{(-1)^{j-1}}{j^{d/2}} z^j \Pi_{aa}(k, \omega; T_a/j), \quad (35)$$

where Π_{aa} denotes the function in the weakly degenerate case derived in the previous sections. We should note here that this result is exact within the convergence radius of the series, i.e., for $z < 1$, while its validity is restricted by the choice of approximation for the fugacity. The first few elements of the series with $j \geq 2$ may be regarded as *quantum corrections* to the nondegenerate result ($j = 1$). We then can write down the quantum correction of the order j for Π as (i.e., shift the index by 1)

$$\Pi_{aa}^{\text{qc}(j)}(k, \omega; T_a) = (-1)^j \frac{2}{n_a \Lambda_a^d} \frac{1}{(j+1)^{d/2}} z^{j+1} \times \Pi_{aa}(k, \omega; T_a/(j+1)). \quad (36)$$

In order to illustrate the results, we consider in this section electrons and holes in bulk Cu₂O. For the fugacity we use the nondegenerate limit $z = n_a \Lambda_a^3/2$. Figure 2 shows the first two quantum correction terms as a function of the wave number q . They are, obviously, tiny for the chosen parameters even though those can be regarded as upper (density) and lower (temperature) bounds, respectively, being relevant for (current) experiments investigating Rydberg excitons [5, 6].

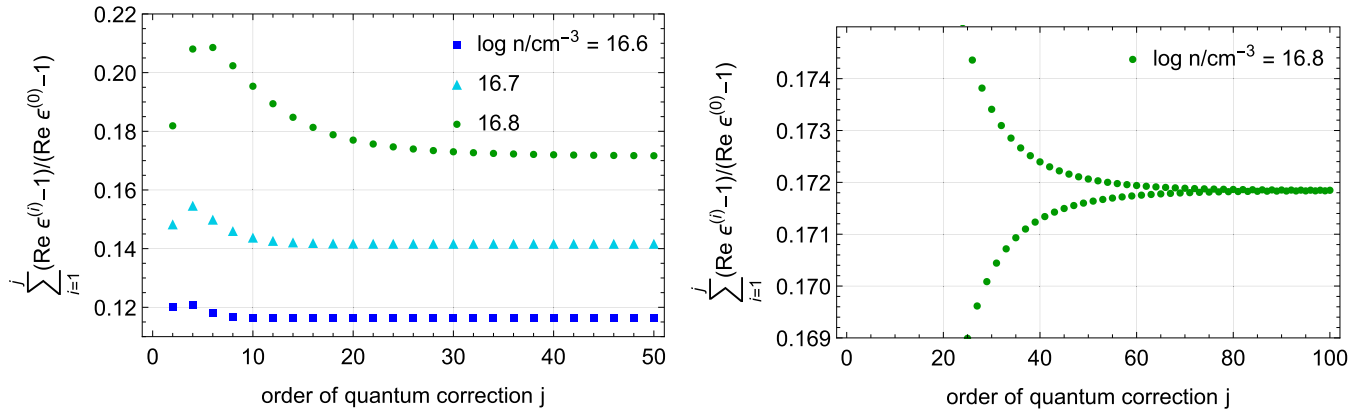


Figure 4. Sum of quantum correction terms up to j th order to the real part of the dielectric function normalized to the nondegenerate term vs order j for a temperature of $T = 10$ K and several carrier densities (left panel). Same quantity only for the highest density, but up to $j = 100$ (right panel).

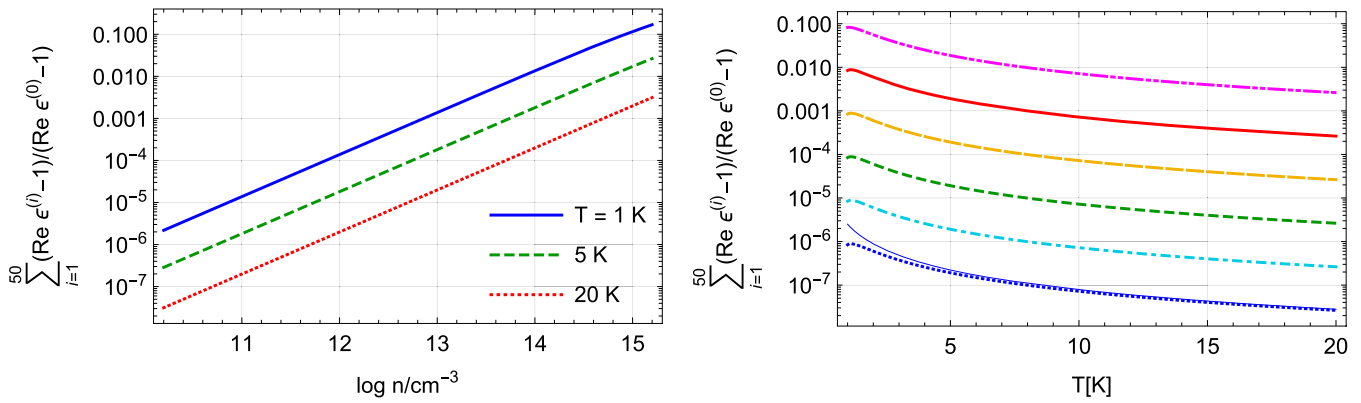


Figure 5. Sum of quantum correction terms up to 50th order to the real part of the dielectric function normalized to the nondegenerate term vs carrier density at a frequency of $\hbar\omega = 5 \mu\text{eV}$ for several temperatures (left panel) and vs temperature for several densities (right panel; from bottom to top: $\log n/\text{cm}^{-3} = 10, 11, 12, 13, 14, 15$). The thin solid blue line in the right-hand panel gives a $T^{-3/2}$ law.

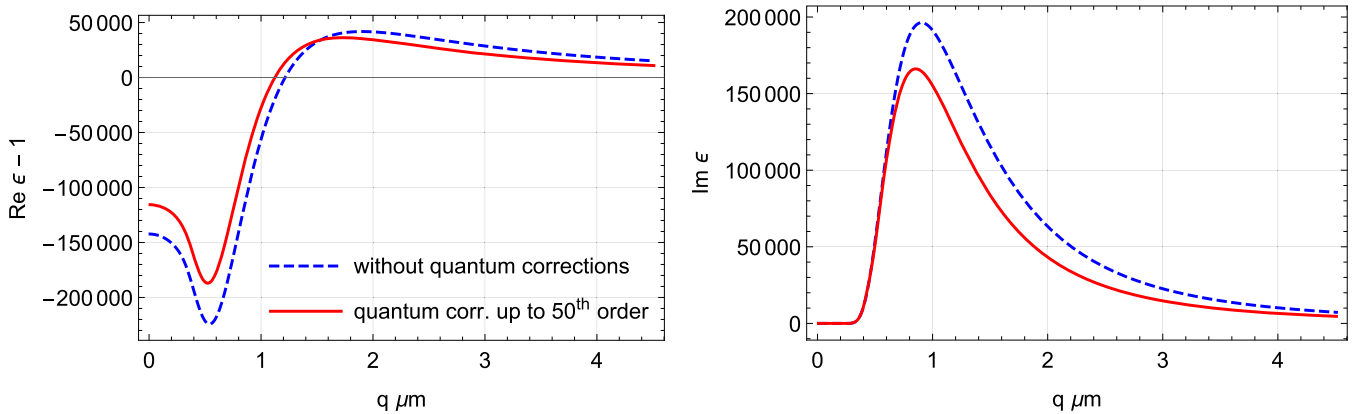


Figure 6. Real part (left panel) and imaginary part (right panel) of the dielectric function vs wave number for a carrier density of $\log n/\text{cm}^{-3} = 16.8$ and a temperature of 10 K. Comparison of nondegenerate term (dashed blue) and quantum corrected function (sum of nondegenerate term and quantum corrections up to 50th order; red).

However, there are situations where the quantum degeneracy is much higher, e.g., in the experiments attempting to prove the existence of an excitonic Bose–Einstein condensate in bulk Cu_2O . There, electron–hole densities around 10^{16} cm^{-3} have been generated by the optical excitation [27].

For the further analysis, we restrict ourselves to the real part and look at the magnitude of the quantum correction terms at fixed wave number and frequency relative to the nondegenerate case, if not given explicitly, at a wave number of $q = 2 \mu\text{m}^{-1}$ and a frequency of $\hbar\omega = 15 \mu\text{eV}$. Figure 3 shows

$(\text{Re } \varepsilon^{(j)} - 1)/(\text{Re } \varepsilon^{(0)} - 1)$ depending on the order j for several densities and temperatures. For a convergent series, the terms have at least to decrease with increasing order which is the case (at $T = 10$ K) only for $\log n/\text{cm}^{-3} \leq 16.8$ (left panel) and (at $\log n/\text{cm}^{-3} = 16.8$) only for $T \geq 10$ K (right panel). Indeed, the border of $n\Lambda^3 = 1/2$ lies for the (lighter) holes with $T = 10$ K just at $\log n/\text{cm}^{-3} = 16.8234$ and with $\log n/\text{cm}^{-3} = 16.8$ just at $T = 9.6472$ K. For densities or temperatures beyond that border, the series (35) is not convergent and the terms (36) have no physical interpretation.

The left panel of figure 4 shows the convergence of the series. It is slower at the border of the coverage area (see also right panel), however, even summing up 100 terms is numerically still quite feasible.

Finally, we consider the sum of quantum correction terms up to 50th order to the real part of the dielectric function normalized to the nondegenerate term as a function of the particle density for several temperatures and vice versa (figure 5). While the density dependence is obviously $\propto n$, the temperature dependence is $\propto T^{-3/2}$, see dashed line in the right panel.

Figure 6 illustrates the effect of quantum corrections on the dielectric function by comparing the weakly degenerate limit and the function including quantum corrections for a system with quantum degeneracy (of the holes) of $\frac{1}{2}n\Lambda_h^3 = 0.95$.

6. Conclusions and outlook

We have derived analytical (RPA) results for the dielectric response of an electron–hole plasma in the weakly-degenerate case and demonstrated that the well-tried result for bulk systems [16] keeps its form also for lower-dimensional structures. Moreover, it is even in the more complicated case of linear carrier dispersion, realized, e.g., in graphene and many topological insulators, possible to derive a result for the polarization function for excited states in an analytical form (see appendix C). Since that function determines, in particular, also the plasmonic properties of bulk and lower-dimensional semiconductors, its knowledge in analytical form can be expected of great usefulness for the calculation of these properties.

In order to generalize the results beyond the weakly-degenerate case, we have established a method which expands the polarization function in a series with respect to the fugacity $z = e^{\beta\mu}$. While the whole series covers the region of weak and moderate degeneracies up to $n\Lambda^d/2 = 1$, its first terms can be regarded as *quantum corrections* to the result in the nondegenerate limit.

For the parameters relevant in the Rydberg exciton experiments in bulk cuprous oxide [5, 6] (ultralow carrier densities of $n \lesssim 10^{12} \text{ cm}^{-3}$), the nondegenerate limit for ε is a very good approximation, and the quantum correction terms are negligible. Obviously, this is not the case for higher densities as in experiments searching for an excitonic Bose–Einstein

condensate [27]. Moreover, one can expect that quantum corrections will play a much more important role in lower-dimensional systems, particularly also in those with Dirac cone functionality.

Acknowledgments

DS gratefully acknowledges support by the Deutsche Forschungsgemeinschaft (Project Number SE 2885/1-1).

Data availability statement

No new data were created or analysed in this study.

Appendix A. Derivation of the effective quasi-two-dimensional Coulomb interaction

Starting point is the effective Coulomb potential between two carriers (electrons and holes) in a quantum well [21],

$$V_{ab}(q) = \frac{e_a e_b}{2\epsilon_0 \epsilon_{b,w} q} \int_{-\infty}^{\infty} dz \int_{-\infty}^{\infty} dz' |\Phi_a(z)|^2 |\Phi_b(z')|^2 \times \exp(-q|z - z'|). \quad (\text{A.1})$$

Here, $\Phi_{a/b}$ are the wave functions of the motion in confinement- (z -)direction, $\epsilon_{b,w}$ is the background dielectric constant in the well, and $e_{e/h} = \mp e$.

The wave functions are those of a particle confined in a one-dimensional quantum well. They read for the case of even (odd) states [28]

$$\Phi_a(z) = \begin{cases} \eta_a B_a \exp\left[\kappa_a \left(z + \frac{d}{2}\right)\right], & -\infty < z \leq -\frac{d}{2} \\ A_a \cos(k_a z), & -\frac{d}{2} \leq z \leq \frac{d}{2} \\ B_a \exp\left[-\kappa_a \left(z - \frac{d}{2}\right)\right], & \frac{d}{2} \leq z < \infty \end{cases} \quad (\text{A.2})$$

with $a = e, h$, $k_a = \left(\frac{2m_{a,w}}{\hbar^2} E\right)^{1/2}$ and $\kappa_a = \left(\frac{2m_{a,b}}{\hbar^2} (V_{0,a} - E)\right)^{1/2}$, $m_{a,w}$ and $m_{a,b}$ being the masses of carrier species a in the well and in the barriers, respectively, $V_{0,a}$ the barrier height, and E the energy of the confined particle. In order to account for even and odd states of electrons and holes, we introduced the factors $\eta_a = \pm 1$ for even (odd) states ($a = e, h$) and the functions

$$\begin{aligned} ct(\theta_a) &= \begin{cases} \cot \theta_a \\ \tan \theta_a, \end{cases} & tc(\theta_a) &= \begin{cases} \tan \theta_a \\ \cot \theta_a, \end{cases} \\ cs(\theta_a) &= \begin{cases} \cos \theta_a \\ \sin \theta_a, \end{cases} & sc(\theta_a) &= \begin{cases} \sin \theta_a \\ \cos \theta_a \end{cases} \end{aligned} \quad (\text{A.3})$$

[upper (lower) functions for even (odd) states].

In order to determine the normalization constants A_a and B_a , we apply the normalization condition of the wave functions,

$$\begin{aligned} 1 &= \int_{-\infty}^{\infty} dz |\Phi_a(z)|^2 \\ &= B_a^2 \int_{-\infty}^{-d/2} dz \exp \left[2\kappa_a \left(z + \frac{d}{2} \right) \right] + A_a^2 \int_{-d/2}^{d/2} dz cs^2(k_a z) \\ &\quad + B_a^2 \int_{d/2}^{\infty} dz \exp \left[-2\kappa_a \left(z - \frac{d}{2} \right) \right] \\ &= \frac{B_a^2}{\kappa_a} + \frac{A_a^2 d}{2} \left(1 + \eta_a \frac{\sin k_a d}{k_a d} \right). \end{aligned} \quad (\text{A.4})$$

Further information can be obtained by making use of the boundary conditions at $z = \pm d/2$, i.e., of the continuity of wave functions and particle fluxes [29]. One gets

$$B_a = A_a cs \left(\frac{k_a d}{2} \right) \quad \text{and} \quad \frac{B_a \kappa_a}{m_{a,b}} = \eta_a \frac{A_a k_a}{m_{a,w}} sc \left(\frac{k_a d}{2} \right). \quad (\text{A.5})$$

The first relation already allows to eliminate one of the two constants. Even more importantly, both relations together lead to

$$\eta_a \frac{m_{a,w} \kappa_a}{m_{a,b} k_a} = tc \left(\frac{k_a d}{2} \right), \quad (\text{A.6})$$

i.e., a condition for the possible energies of the particle's motion in z -direction. The solutions can be illustrated most easily by abbreviating

$$\begin{aligned} \theta_a &= \frac{k_a d}{2}, \quad \theta_{a,0} = \frac{k_{a,0} d}{2}, \\ k_{a,0} &= \left(\frac{2m_{a,w}}{\hbar^2} V_{0,a} \right)^{1/2}, \quad \alpha_a = \frac{m_{a,w}}{m_{a,b}} \end{aligned} \quad (\text{A.7})$$

which renders (A.6) into

$$\eta_a \sqrt{\alpha_a} \left(\frac{\theta_{a,0}^2}{\theta_a^2} - 1 \right)^{1/2} = tc(\theta_a). \quad (\text{A.8})$$

We proceed now with the further evaluation of (A.4). Inserting (A.5)–(A.7) one obtains

$$1 = \frac{A_a^2 d}{2} \left[1 + \eta_a \frac{\alpha_a}{\theta_a} ct(\theta_a) + \eta_a \frac{1 - \alpha_a}{\theta_a} \cos \theta_a \sin \theta_a \right], \quad (\text{A.9})$$

i.e., the normalization constant A_a follows to be

$$A_a = \left(\frac{2}{d} \right)^{1/2} \frac{1}{\left(1 + \eta_a \frac{\alpha_a}{\theta_a} ct(\theta_a) + \eta_a \frac{1 - \alpha_a}{\theta_a} \cos \theta_a \sin \theta_a \right)^{1/2}}. \quad (\text{A.10})$$

Now we go back to (A.1). Inserting the wave function (A.2), the potential consists of three parts,

$$V_{ab}(q) = \frac{e_a e_b}{2\epsilon_0 \epsilon_{b,w} q} (I_1 + I_2 + I_3) \quad (\text{A.11})$$

with

$$\begin{aligned} I_1 &= B_a^2 B_b^2 \int_{-\infty}^{-d/2} dz \int_{-\infty}^{-d/2} dz' \exp \left[2\kappa_a \left(z + \frac{d}{2} \right) \right] \\ &\quad \times \exp \left[2\kappa_b \left(z' + \frac{d}{2} \right) \right] \exp(-q|z - z'|) \\ &= B_a^2 B_b^2 \left\{ \int_{-\infty}^{-d/2} dz' \int_{-\infty}^{z'} dz \exp \left[2\kappa_a \left(z + \frac{d}{2} \right) \right] \right. \\ &\quad \times \exp \left(2\kappa_b \left(z' + \frac{d}{2} \right) \right) \exp[-q(z' - z)] \\ &\quad + \int_{-\infty}^{-d/2} dz' \int_{z'}^{-d/2} dz \exp \left[2\kappa_a \left(z + \frac{d}{2} \right) \right] \\ &\quad \times \exp \left[2\kappa_b \left(z' + \frac{d}{2} \right) \right] \exp[-q(z - z')] \left. \right\} \\ &= B_a^2 B_b^2 \frac{\kappa_a + \kappa_b + q}{(\kappa_a + \kappa_b)(2\kappa_a + q)(2\kappa_b + q)}. \end{aligned} \quad (\text{A.12})$$

Using the relation (A.6) and the abbreviations (A.7) (furthermore $Q = qd/2$), and inserting (A.5) and (A.10), one arrives at

$$\begin{aligned} I_1 &= \frac{\alpha_a \alpha_b cs^2(\theta_a) cs^2(\theta_b)}{\left(1 + \eta_a \frac{\alpha_a}{\theta_a} ct(\theta_a) + \eta_a \frac{1 - \alpha_a}{\theta_a} \cos \theta_a \sin \theta_a \right) \left(1 + \eta_b \frac{\alpha_b}{\theta_b} ct(\theta_b) + \eta_b \frac{1 - \alpha_b}{\theta_b} \cos \theta_b \sin \theta_b \right)} \\ &\quad \times \frac{\eta_a \alpha_b \theta_a tc(\theta_a) + \eta_b \alpha_a \theta_b tc(\theta_b) + \alpha_a \alpha_b Q}{(\eta_a \alpha_b \theta_a tc(\theta_a) + \eta_b \alpha_a \theta_b tc(\theta_b))(2\eta_a \theta_a tc(\theta_a) + \alpha_a Q)(2\eta_b \theta_b tc(\theta_b) + \alpha_b Q)}. \end{aligned} \quad (\text{A.13})$$

The calculation of I_3 runs analogously with the result $I_3 = I_1$. For I_2 one gets

$$I_2 = A_a^2 A_b^2 \int_{-d/2}^{d/2} dz \int_{-d/2}^{d/2} dz' cs^2(k_a z) cs^2(k_b z') \exp(-q|z - z'|)$$

$$\begin{aligned} &= \frac{d}{2q} A_a^2 A_b^2 \left\{ 1 + \eta_a \frac{\sin(k_a d)}{k_a d} + \eta_b \frac{q^2}{4k_b^2 + q^2} \right. \\ &\quad \times \left[\frac{\sin(k_b d)}{k_b d} + \eta_a \frac{\sin((k_a + k_b)d)}{2(k_a + k_b)d} + \eta_a \frac{\sin((k_a - k_b)d)}{2(k_a - k_b)d} \right] \end{aligned}$$

$$\begin{aligned}
& -\frac{1}{qd} \left[1 - e^{-qd} + \eta_a \frac{q^2}{4k_a^2 + q^2} (\cos(k_a d) (1 - e^{-qd}) \right. \\
& \left. + \frac{2k_a}{q} \sin(k_a d) (1 + e^{-qd}) \right) \times \left[1 + \eta_b \frac{q^2}{4k_b^2 + q^2} \left(\cos(k_b d) - \frac{2k_b}{q} \sin(k_b d) \right) \right] \Bigg\}.
\end{aligned}
\tag{A.14}$$

Using now again the relations (A.6) and (A.10) and the abbreviations (A.7) and $Q = qd/2$, one finally arrives at

$$\begin{aligned}
I_2 = & \frac{1}{Q} \frac{1}{\left(1 + \eta_a \frac{\alpha_a}{\theta_a} ct(\theta_a) + \eta_a \frac{1-\alpha_a}{\theta_a} \cos \theta_a \sin \theta_a \right) \left(1 + \eta_b \frac{\alpha_b}{\theta_b} ct(\theta_b) + \eta_b \frac{1-\alpha_b}{\theta_b} \cos \theta_b \sin \theta_b \right)} \\
& \times \left\{ 1 + \eta_a \frac{\sin(2\theta_a)}{2\theta_a} + \eta_b \frac{Q^2}{4\theta_b^2 + Q^2} \left[\frac{\sin(2\theta_b)}{2\theta_b} + \eta_a \frac{\sin(2(\theta_a + \theta_b))}{4(\theta_a + \theta_b)} + \eta_a \frac{\sin(2(\theta_a - \theta_b))}{4(\theta_a - \theta_b)} \right] \right. \\
& - \frac{1}{2Q} \left[1 - e^{-2Q} + \eta_a \frac{Q^2}{4\theta_a^2 + Q^2} \left(\cos(2\theta_a) (1 - e^{-2Q}) + \frac{2\theta_a}{Q} \sin(2\theta_a) (1 + e^{-2Q}) \right) \right] \\
& \left. \times \left[1 + \eta_b \frac{Q^2}{4\theta_b^2 + Q^2} \left(\cos(2\theta_b) - \frac{2\theta_b}{Q} \sin(2\theta_b) \right) \right] \right\}.
\end{aligned}
\tag{A.15}$$

We insert the results for $I_1 = I_3$ and I_2 into (A.11) and obtain for the effective Coulomb interaction in a quantum well

$$\begin{aligned}
V_{ab}(Q) = & \frac{de_a e_b}{4\epsilon_0 \epsilon_{b,w} Q} \frac{1}{\left(1 + \eta_a \frac{\alpha_a}{\theta_a} ct(\theta_a) + \eta_a \frac{1-\alpha_a}{\theta_a} \cos \theta_a \sin \theta_a \right) \left(1 + \eta_b \frac{\alpha_b}{\theta_b} ct(\theta_b) + \eta_b \frac{1-\alpha_b}{\theta_b} \cos \theta_b \sin \theta_b \right)} \\
& \times \left(\frac{\alpha_a \alpha_b cs^2(\theta_a) cs^2(\theta_b) (\eta_a \alpha_b \theta_a tc(\theta_a) + \eta_b \alpha_a \theta_b tc(\theta_b) + \alpha_a \alpha_b Q)}{(\eta_a \alpha_b \theta_a tc(\theta_a) + \eta_b \alpha_a \theta_b tc(\theta_b)) (2\eta_a \theta_a tc(\theta_a) + \alpha_a Q) (2\eta_b \theta_b tc(\theta_b) + \alpha_b Q)} \right. \\
& + \frac{1}{Q} \left\{ 1 + \eta_a \frac{\sin(2\theta_a)}{2\theta_a} + \eta_b \frac{Q^2}{4\theta_b^2 + Q^2} \left[\frac{\sin(2\theta_b)}{2\theta_b} + \eta_a \frac{\sin(2(\theta_a + \theta_b))}{4(\theta_a + \theta_b)} + \eta_a \frac{\sin(2(\theta_a - \theta_b))}{4(\theta_a - \theta_b)} \right] \right. \\
& - \frac{1}{2Q} \left[1 - e^{-2Q} + \eta_a \frac{Q^2}{4\theta_a^2 + Q^2} \left(\cos(2\theta_a) (1 - e^{-2Q}) + \frac{2\theta_a}{Q} \sin(2\theta_a) (1 + e^{-2Q}) \right) \right] \\
& \left. \left. \times \left[1 + \eta_b \frac{Q^2}{4\theta_b^2 + Q^2} \left(\cos(2\theta_b) - \frac{2\theta_b}{Q} \sin(2\theta_b) \right) \right] \right\} \right).
\end{aligned}
\tag{A.16}$$

For illustration we consider the case of GaAs quantum wells embedded in $\text{Al}_x\text{Ga}_{1-x}\text{As}$ barriers. This system has the following parameters [30, 31]: electron masses $m_{e,w} = 0.063m_0$ and $m_{e,b} = (0.063 + 0.083x)m_0$, hole masses $m_{h,w} = 0.51m_0$ and $m_{h,b} = (0.51 + 0.25x)m_0$ (i.e., $\alpha_e = 0.717$ and $\alpha_h = 0.872$), dielectric constants $\epsilon_{b,w} = 12.90$ and $\epsilon_{b,b} = 12.90 - 2.84x$, and energy gap mismatch $\Delta E_g = 365.5$ meV (which splits onto electrons and holes like 0.65/0.35 so that $V_{0,e} = 237.575$ meV and $V_{0,h} = 127.925$ meV). We use in the following $x = 0.3$ and a well width of $d = 20$ nm.

Figure A1 shows the graphical solution of (A.8). The electrons exhibit three even and two odd bound states, the holes exhibit six even and five odd bound states. Remember that $d = 20$ nm here. The number of bound states increases with increasing well width.

The effective Coulomb potential (A.11) is shown in figure A2 for various even electron bound states in the well. [Keep in mind that here single-particle bound states in the well are meant. They must not be confused with electron-hole (two-particle) bound states, i.e. excitons.] We denote them by

the quantum number pairs $[e, e]$ with $e = 1, 2, 3$. Remember that $Q = qd/2$ in (A.11).

In the right panel, the effective potential is compared to the limiting cases for two ($V_{ee}^{2d} \propto 1/q$) and three dimensions ($V_{ee}^{3d} \propto 1/q^2$).

Appendix B. Derivation of the polarization function in the one-dimensional case

In a 1d system, the polarization function is given by

$$\Pi_{aa}^{(1d)}(k, \omega) = \frac{1}{2\pi} n_a \Lambda_a \exp\left(-\frac{\hbar^2 k^2}{8m_a k_B T_a}\right) I \tag{B.1}$$

with

$$\begin{aligned}
I = & \int_{-\infty}^{\infty} dq e^{-\beta a q^2} (e^{\beta a k q} - e^{-\beta a k q}) \\
& \times \left[\frac{w - 2akq}{(w - 2ax)^2 + \epsilon^2} - \frac{i\epsilon}{(w - 2akq)^2 + \epsilon^2} \right] \\
= & I_1 + I_2.
\end{aligned}
\tag{B.2}$$

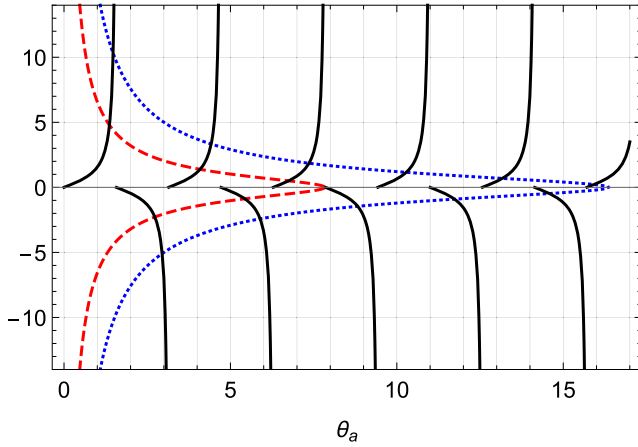


Figure A1. Graphical solution of (A.8) for even (above the abscissa) and odd states (below the abscissa): rhs (black solid lines) and lhs for electrons (red dashed), and holes (blue dotted).

We introduce the abbreviations $x = akq$ and $u = \beta/(ak^2)$ making the integral easier readable,

$$I = \frac{1}{ak} \int_{-\infty}^{\infty} dx e^{-ux^2} (e^{\beta x} - e^{-\beta x}) \times \left[\frac{w - 2x}{(w - 2x)^2 + \epsilon^2} - \frac{i\epsilon}{(w - 2x)^2 + \epsilon^2} \right] = I_1 + I_2. \quad (\text{B.3})$$

The second (imaginary) contribution I_2 can again be calculated straightforwardly. Performing the limit $\epsilon \rightarrow 0$ leads to

$$I_2 = -\frac{i\pi}{ak} \int_{-\infty}^{\infty} dx e^{-ux^2} (e^{\beta x} - e^{-\beta x}) \delta(w - 2x) = -\frac{i\pi}{2ak} \exp\left(-\frac{\beta w^2}{4ak^2}\right) \left[\exp\left(\frac{\beta w}{2}\right) - \exp\left(-\frac{\beta w}{2}\right) \right]. \quad (\text{B.4})$$

In the first (real) contribution to I (B.3) we proceed as before applying the integration trick (14),

$$I_1 = \frac{1}{ak} \int_{-\infty}^{\infty} dx e^{-ux^2} (e^{\beta x} - e^{-\beta x}) (w - 2x) \times \int_0^{\infty} dz \exp[(w - 2x)^2 + \epsilon^2]z) = \frac{1}{ak} \int_0^{\infty} dz \exp(-(w^2 + \epsilon^2)z) \int_{-\infty}^{\infty} dx \exp(-(u + 4z)x^2) \times (e^{(\beta+4z)x} - e^{-(\beta-4z)x}) (w - 2x) = \frac{1}{ak} \int_0^{\infty} dz \exp((w^2 + \epsilon^2)z) I_1^{(xy)}(z). \quad (\text{B.5})$$

The result of the x - and y -integrations is simple compared to the 2d case,

$$I_1^{(xy)}(z) = \frac{\sqrt{\pi}}{(u + 4z)^{3/2}} \left\{ (uw - \beta) \exp\left[\frac{(\beta + 4wz)^2}{4(u + 4z)}\right] - (uw + \beta) \exp\left[\frac{(\beta - 4wz)^2}{4(u + 4z)}\right] \right\}. \quad (\text{B.6})$$

We insert (B.6) into (B.5) and perform the limit $\epsilon \rightarrow 0$, yielding finally

$$I_1 = \frac{\sqrt{\pi}}{ak} \int_0^{\infty} dz e^{-w^2 z} \frac{1}{(u + 4z)^{3/2}} \times \left\{ (uw - \beta) \exp\left[\frac{(\beta + 4wz)^2}{4(u + 4z)}\right] - (uw + \beta) \exp\left[\frac{(\beta - 4wz)^2}{4(u + 4z)}\right] \right\} = \frac{\sqrt{\pi}}{ak} \exp\left(\frac{\beta^2}{4u}\right) \left[F\left(\frac{uw - \beta}{2\sqrt{u}}\right) - F\left(\frac{uw + \beta}{2\sqrt{u}}\right) \right] = \frac{\sqrt{\pi}}{ak} \exp\left(\frac{\beta ak^2}{4}\right) \left\{ F\left[\frac{\sqrt{\beta}}{2\sqrt{ak}}(w - ak^2)\right] - F\left[\frac{\sqrt{\beta}}{2\sqrt{ak}}(w + ak^2)\right] \right\} \quad (\text{B.7})$$

with Dawson's integral F .

Therefore, the final result for the sum of real and imaginary parts again can be expressed in terms of the Faddeeva function w ,

$$e^{-\frac{\beta ak^2}{4}} I = e^{-\frac{\beta ak^2}{4}} (I_1 + I_2) = -\frac{\pi}{2ak} \left(\frac{2}{\sqrt{\pi}} \left\{ F\left[\frac{\sqrt{\beta}}{2\sqrt{ak}}(w + ak^2)\right] - F\left[\frac{\sqrt{\beta}}{2\sqrt{ak}}(w - ak^2)\right] \right\} + i \left\{ \exp\left[-\frac{\beta}{4ak^2}(w - ak^2)^2\right] - \exp\left[-\frac{\beta}{4ak^2}(w + ak^2)^2\right] \right\} \right) = \frac{i\pi}{2ak} \left\{ w \left[\frac{\sqrt{\beta}}{2\sqrt{ak}}(w + ak^2) \right] - w \left[\frac{\sqrt{\beta}}{2\sqrt{ak}}(w - ak^2) \right] \right\}, \quad (\text{B.8})$$

and the polarization function reads

$$\Pi_{aa}^{(1d)}(k, \omega) = \frac{1}{(2\pi)^2} n_a \Lambda_a \frac{i\pi}{2ak} \left\{ w \left[\frac{\sqrt{\beta}}{2\sqrt{ak}}(w + ak^2) \right] - w \left[\frac{\sqrt{\beta}}{2\sqrt{ak}}(w - ak^2) \right] \right\} = i \frac{\sqrt{\pi}}{2} n_a \sqrt{\frac{2m_a}{\hbar^2 k^2}} \frac{1}{\sqrt{k_B T_a}} \times \left\{ w \left[\frac{1}{2\sqrt{k_B T_a}} \sqrt{\frac{2m_a}{\hbar^2 k^2}} \left(\hbar\omega + \frac{\hbar^2 k^2}{2m_a} \right) \right] - w \left[\frac{1}{2\sqrt{k_B T_a}} \sqrt{\frac{2m_a}{\hbar^2 k^2}} \left(\hbar\omega - \frac{\hbar^2 k^2}{2m_a} \right) \right] \right\}. \quad (\text{B.9})$$

Comparing this with the 3d and 2d results (20) and (30), we find that $\Pi_{aa}^{(1d)}(k, \omega) = \Pi_{aa}^{(2d)}(k, \omega) = \Pi_{aa}^{(3d)}(k, \omega)$.

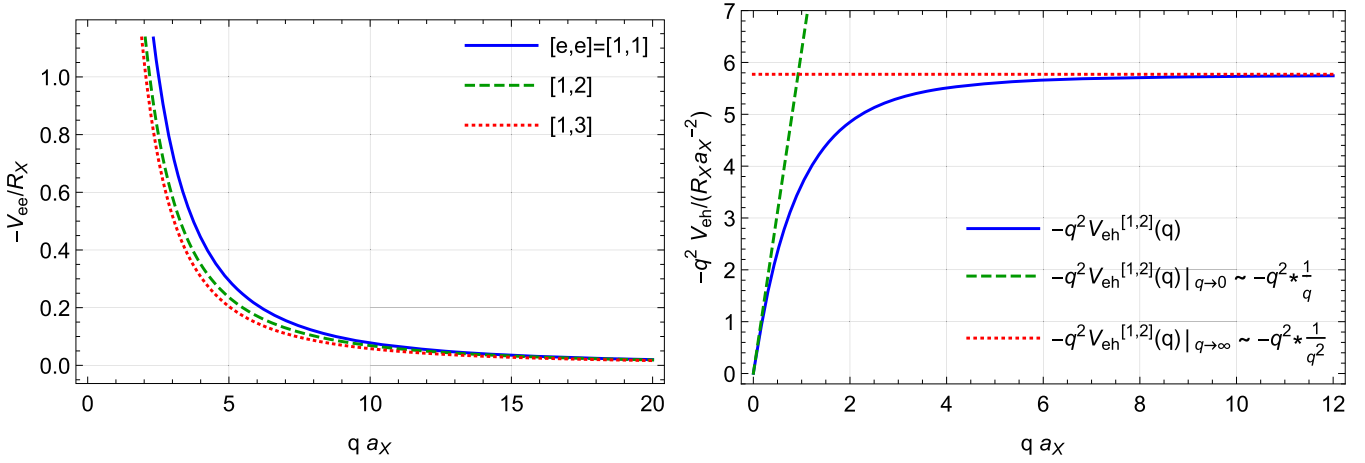


Figure A2. Left panel: effective quasi-two-dimensional Coulomb potential (A.11) between even states of electrons vs wave number q (a_X is the (3d) excitonic Bohr radius and R_X the (3d) excitonic Rydberg energy), right panel: same quantity times square of the wave number q compared to the 2d and 3d limiting cases.

Appendix C. Derivation of the polarization function for linear carrier dispersion

We consider the case of quasi-two-dimensional systems with linear carrier dispersions, $E(\mathbf{k}) = \gamma k$, without an energy gap between ‘valence’ and ‘conduction’ band which resemble the Dirac cones of relativistic massless fermions. In such a system, interband transitions have to be taken into account, and the expression for the dielectric function (1) has to be modified into

$$\varepsilon(k, \omega) = 1 - V_{ee}(k) \sum_{a,b} \Pi_{ab}(k, \omega) \quad (\text{C.1})$$

where $a, b = \pm 1$ denote electrons in the upper (+) and lower (−) cone, respectively. The polarization function reads

$$\begin{aligned} \Pi_{ab}(k, \omega) &= \frac{2}{(2\pi)^2} \int d^2 q \mathcal{F}_{ab}(\mathbf{k}, \mathbf{q}) \\ &\times \frac{f_b\left(\left|\frac{\mathbf{k}}{2} - \mathbf{q}\right|\right) - f_a\left(\left|\frac{\mathbf{k}}{2} + \mathbf{q}\right|\right)}{w + E_b\left(\left|\frac{\mathbf{k}}{2} - \mathbf{q}\right|\right) - E_a\left(\left|\frac{\mathbf{k}}{2} + \mathbf{q}\right|\right) + i\epsilon} \\ &= \frac{1}{2\pi^2} \left\{ \mathcal{P} \int d^2 q \mathcal{F}_{ab}(\mathbf{k}, \mathbf{q}) \right. \\ &\times \frac{f_b\left(\left|\frac{\mathbf{k}}{2} - \mathbf{q}\right|\right) - f_a\left(\left|\frac{\mathbf{k}}{2} + \mathbf{q}\right|\right)}{w + E_b\left(\left|\frac{\mathbf{k}}{2} - \mathbf{q}\right|\right) - E_a\left(\left|\frac{\mathbf{k}}{2} + \mathbf{q}\right|\right)} \\ &- i\pi \int d^2 q \mathcal{F}_{ab}(\mathbf{k}, \mathbf{q}) \\ &\times \left[f_b\left(\left|\frac{\mathbf{k}}{2} - \mathbf{q}\right|\right) - f_a\left(\left|\frac{\mathbf{k}}{2} + \mathbf{q}\right|\right) \right] \\ &\times \delta\left(w + E_b\left(\left|\frac{\mathbf{k}}{2} - \mathbf{q}\right|\right) - E_a\left(\left|\frac{\mathbf{k}}{2} + \mathbf{q}\right|\right)\right) \left. \right\}. \end{aligned} \quad (\text{C.2})$$

The band overlap factor $\mathcal{F}_{ab}(\mathbf{k}, \mathbf{q})$ arises from degenerate bands like in graphene, i.e.,

$$\mathcal{F}_{ab}(\mathbf{k}, \mathbf{q}) = \begin{cases} \frac{1}{2}(1 + ab \cos \theta_{\mathbf{q}, \mathbf{k}+\mathbf{q}}) & \text{if band overlap} \\ & \text{is considered} \\ 1 & \text{otherwise.} \end{cases} \quad (\text{C.3})$$

Obviously, the energy differences are given by

$$E_{\pm}(k) - E_{\pm}(k') = \pm\gamma(k - k'), \quad E_{\pm}(k) - E_{\mp}(k') = \pm\gamma(k + k'), \quad (\text{C.4})$$

i.e., $E_b(k) - E_a(k') = b\gamma(k - abk')$. Concerning the occupation of the bands we consider the case of weak excitation above the ground state with $\mu = 0$, i.e., a small number of electrons is excited from the lower into the upper cone, e.g., by a laser. Then we have in the upper cone an electron distribution which can be well approximated by a Boltzmann distribution, $f_+(k) \approx \frac{n\Lambda^2}{2} e^{-\beta\gamma k}$, and the distribution of the electrons in the lower cone is given by $f_-(k) = 1 - f_+(k) \approx 1 - \frac{n\Lambda^2}{2} e^{-\beta\gamma k}$.

First we look at the imaginary part of Π_{ab} (last summand of (C.2)). After inserting the distribution function and energy differences, the expression does not look much more complicated than in the case of parabolic dispersion (cf (9)), however, the absolute values of wave number differences turn into square roots, and the expression cannot be integrated straightforwardly. Instead, we first introduce an additional auxiliary integration by substituting the variables

$$\gamma\left(\frac{\mathbf{k}}{2} - \mathbf{q}\right) = \mathbf{x}, \quad \gamma\left(\frac{\mathbf{k}}{2} + \mathbf{q}\right) = \mathbf{y}, \quad \text{i.e., } \mathbf{x} + \mathbf{y} = \gamma\mathbf{k}. \quad (\text{C.5})$$

$\text{Im } \Pi_{ab}$ then reads

$$\begin{aligned} \text{Im } \Pi_{ab}(k, \omega) &= -\frac{1}{2\pi\gamma^2} \int d^2 x \int d^2 y [f_b(x) - f_a(y)] \mathcal{F}_{ab}(\mathbf{x}, \mathbf{y}) \\ &\times \delta[w + b(x - aby)] \delta(\mathbf{y} - (\gamma\mathbf{k} - \mathbf{x})) \end{aligned} \quad (\text{C.6})$$

with

$$\mathcal{F}_{ab}(\mathbf{x}, \mathbf{y}) = \mathcal{F}_{ab}(x, y, \cos \varphi)$$

$$= \begin{cases} \frac{1}{2}(1 + ab \cos \theta_{-\mathbf{x}, \gamma \mathbf{k} - \mathbf{x}}) \\ \frac{1}{2} \left[1 + ab \frac{\gamma k \cos \varphi}{(\gamma^2 k^2 + x^2 - 2\gamma k x \cos \varphi)^{1/2}} \right] \\ 1 \end{cases} \quad (\text{C.7})$$

(see (C.3)), where $\varphi = \varphi_x = \angle(\mathbf{k}, \mathbf{x})$.

The expression (C.6) is easier to handle, however, the last delta function has to be considered very carefully. We introduce polar coordinates (the abscissa for the x -integration is chosen in k -direction):

$$\begin{aligned} \text{Im } \Pi_{ab}(k, \omega) &= -\frac{1}{2\pi\gamma^2} \int_0^\infty dx x \int_0^\infty dy y \int_0^{2\pi} d\varphi_x \int_0^{2\pi} d\varphi_y \\ &\quad \times [f_b(x) - f_a(y)] \mathcal{F}_{ab}(x, y, \cos \varphi_x) \\ &\quad \times \delta[w + b(x - aby)] \frac{1}{y} \delta(y - |\gamma \mathbf{k} - \mathbf{x}|) \delta(\varphi_y - \varphi_x) \\ &= -\frac{1}{2\pi\gamma^2} \int_0^\infty dx x \int_0^\infty dy y \int_0^{2\pi} d\varphi [f_b(x) - f_a(y)] \\ &\quad \times \mathcal{F}_{ab}(x, y, \cos \varphi) \delta[w + b(x - aby)] \\ &\quad \times \delta \left[y - (\gamma^2 k^2 + x^2 - 2\gamma k x \cos \varphi)^{1/2} \right]. \end{aligned} \quad (\text{C.8})$$

To perform the φ -integration we use the last delta function,

$$\begin{aligned} &\delta \left[y - (\gamma^2 k^2 + x^2 - 2\gamma k x \cos \varphi)^{1/2} \right] \\ &= \sum_{i=1}^2 \frac{1}{|f'(\varphi)|_{\varphi=\varphi_i}} \delta(\varphi - \varphi_i) \end{aligned} \quad (\text{C.9})$$

with

$$\begin{aligned} \cos \varphi_{1/2} &= \frac{1}{2\gamma k x} (\gamma^2 k^2 + x^2 - y^2), \\ |f'(\varphi)| &= \frac{\gamma k x |\sin \varphi|}{(\gamma^2 k^2 + x^2 - 2\gamma k x \cos \varphi)^{1/2}}, \end{aligned} \quad (\text{C.10})$$

$$|f'(\varphi)|_{\varphi=\varphi_{1/2}} = \frac{\{[(x+y)^2 - \gamma^2 k^2][\gamma^2 k^2 - (x-y)^2]\}^{1/2}}{2y}.$$

From the conditions for real solutions (i) $|\cos \varphi_{1/2}| \leq 1$ and (ii) positive radicand in the last line of (C.10), we find the restriction $|\gamma k - x| \leq y \leq \gamma k + x$.

Inserting now (C.9) and (C.10) into (C.8), we obtain

$$\begin{aligned} \text{Im } \Pi_{ab}(k, \omega) &= -\frac{2}{\pi\gamma^2} \int_0^\infty dx \int_{|\gamma k - x|}^{\gamma k + x} dy [f_b(x) - f_a(y)] \\ &\quad \times \delta[w + b(x - aby)] \\ &\quad \times \frac{xy \mathcal{F}_{ab}(x, y)}{\{[(x+y)^2 - \gamma^2 k^2][\gamma^2 k^2 - (x-y)^2]\}^{1/2}} \end{aligned} \quad (\text{C.11})$$

with

$$\mathcal{F}_{ab}(x, y) = \begin{cases} \frac{1}{2} \left[1 + \frac{ab}{2xy} (\gamma^2 k^2 - x^2 - y^2) \right] \\ 1. \end{cases} \quad (\text{C.12})$$

Introducing dimensionless sum and difference variables, $z = (x+y)/(\gamma k)$ and $t = (y-x)/(\gamma k)$, respectively, and abbreviating $u = \beta\gamma k/2$ and $v = w/(\gamma k)$, (C.11) turns into

$$\begin{aligned} \text{Im } \Pi_{ab}(k, \omega) &= -\frac{1}{\pi\gamma^2} \frac{\gamma k}{4} \int_1^\infty dz \int_{-1}^1 dt \\ &\quad \times \left[f_b \left(\frac{z-t}{2} \right) - f_a \left(\frac{z+t}{2} \right) \right] \\ &\quad \times \delta \left(v - b \left\{ \frac{t}{z} \right\} \right) \frac{(z^2 - t^2) \mathcal{F}_{ab}(z, t)}{[(z^2 - 1)(1 - t^2)]^{1/2}} \end{aligned} \quad (\text{C.13})$$

with

$$\mathcal{F}_{ab}(z, t) = \begin{cases} \frac{z^2 - 1}{z^2 - t^2} & , \quad ab = +1, \text{ intraband transitions} \\ \frac{1 - t^2}{z^2 - t^2} & , \quad ab = -1, \text{ interband transitions} \\ 1 & , \quad \text{no band overlap considered,} \end{cases} \quad (\text{C.14})$$

so that the last fraction in (C.13) reads

$$\frac{(z^2 - t^2) \mathcal{F}_{ab}(z, t)}{[(z^2 - 1)(1 - t^2)]^{1/2}} = \begin{cases} \left[\frac{z^2 - 1}{1 - t^2} \right]^{1/2} & , \quad ab = +1, \text{ intraband} \\ \left[\frac{1 - t^2}{z^2 - 1} \right]^{1/2} & , \quad ab = -1, \text{ interband} \\ \left[\frac{z^2 - 1}{1 - t^2} \right]^{1/2} + \left[\frac{1 - t^2}{z^2 - 1} \right]^{1/2} & , \quad \text{no band overlap.} \end{cases} \quad (\text{C.15})$$

In the following, we consider the case with band overlap only. Inserting (C.15) and the difference of distribution functions into (C.13), we obtain for the intraband contributions to $\text{Im } \Pi$

$$\begin{aligned} \text{Im } \Pi_{++}(k, \omega) &= -\frac{n\Lambda^2}{\pi\gamma^2} \frac{\gamma k}{8} \int_1^\infty dz e^{-uz} \sqrt{z^2 - 1} \\ &\quad \times \int_{-1}^1 dt \frac{e^{ut} - e^{-ut}}{\sqrt{1-t^2}} \delta(v-t) \\ &= -\frac{n\Lambda^2}{\pi\gamma^2} \frac{\gamma k}{8} \frac{K_1(u)}{u} \frac{e^{uv} - e^{-uv}}{\sqrt{1-v^2}} \Theta(1-v)\Theta(1+v) \\ &= \text{Im } \Pi_{--}(k, \omega), \end{aligned} \quad (\text{C.16})$$

where K_0 and K_1 denote modified Bessel functions of the second kind, also referred to as MacDonald functions or modified Hankel functions (i.e., Hankel functions with imaginary arguments, $K_\nu(x) = \frac{\pi}{2} i^{\nu+1} H_\nu^{(1)}(ix)$ [17]). For the interband contributions we get

$$\begin{aligned} \text{Im } \Pi_{+-}(k, \omega) &= \frac{n\Lambda^2}{\pi\gamma^2} \frac{\gamma k}{8} \int_1^\infty dz \frac{e^{-uz}}{\sqrt{z^2 - 1}} \delta(v-z) \\ &\quad \times \int_{-1}^1 dt [e^{ut} + e^{-ut}] \sqrt{1-t^2} \\ &\quad - \frac{1}{\pi\gamma^2} \frac{\gamma k}{4} \int_1^\infty dz \frac{1}{\sqrt{z^2 - 1}} \delta(v-z) \int_{-1}^1 dt \sqrt{1-t^2} \\ &= \frac{1}{\gamma^2} \frac{\gamma k}{4} \left\{ n\Lambda^2 \frac{e^{-uv}}{\sqrt{v^2 - 1}} \frac{I_1(u)}{u} \right. \\ &\quad \left. - \frac{1}{2} \frac{1}{\sqrt{v^2 - 1}} \right\} \Theta(v-1), \end{aligned} \quad (\text{C.17})$$

$$\begin{aligned} \text{Im } \Pi_{-+}(k, \omega) &= -\frac{n\Lambda^2}{\pi\gamma^2} \frac{\gamma k}{8} \int_1^\infty dz \frac{e^{-uz}}{\sqrt{z^2 - 1}} \delta(v+z) \\ &\quad \times \int_{-1}^1 dt [e^{ut} + e^{-ut}] \sqrt{1-t^2} \\ &\quad + \frac{1}{\pi\gamma^2} \frac{\gamma k}{4} \int_1^\infty dz \frac{1}{\sqrt{z^2 - 1}} \delta(v+z) \int_{-1}^1 dt \sqrt{1-t^2} \\ &= -\frac{1}{\gamma^2} \frac{\gamma k}{4} \left\{ n\Lambda^2 \frac{e^{-uv}}{\sqrt{v^2 - 1}} \frac{I_1(u)}{u} \right. \\ &\quad \left. - \frac{1}{2} \frac{1}{\sqrt{v^2 - 1}} \right\} \Theta(-v-1), \end{aligned} \quad (\text{C.18})$$

where I_n denotes the modified Bessel function of first kind (i.e., Bessel functions with imaginary arguments, $I_\nu(x) = i^{-\nu} J_\nu(ix)$) [17].

Looking back at (C.15), in the case without band overlap, there would occur the double number of terms in the contributions to $\text{Im } \Pi$ considered above. However, the additional terms

lead to divergencies which casts the physical sense of this case into doubt.

The real part of the polarization function can be obtained either via Kramers–Kronig transformation of the imaginary part or, equivalently, directly from (C.2). Since the calculation runs analogously, we have only to replace the remaining delta functions in (C.13) or (C.16)–(C.18), respectively, by the corresponding denominator, e.g., $\delta(v-t) \rightarrow \frac{1}{v-t}$ etc. Obviously, then one integral remains in each case,

$$\begin{aligned} \text{Re } \Pi_{++}(k, \omega) &= \frac{n\Lambda^2}{\pi^2\gamma^2} \frac{\gamma k}{8} \frac{K_1(u)}{u} \mathcal{P} \int_{-1}^1 dt \frac{e^{ut} - e^{-ut}}{\sqrt{1-t^2}} \frac{1}{v-t} \\ &= \text{Re } \Pi_{--}(k, \omega), \end{aligned} \quad (\text{C.19})$$

$$\begin{aligned} \text{Re } \Pi_{+-}(k, \omega) &= -\frac{1}{\pi\gamma^2} \frac{\gamma k}{4} \left\{ n\Lambda^2 \frac{I_1(u)}{u} \mathcal{P} \int_1^\infty dz \frac{e^{-uz}}{\sqrt{z^2 - 1}} \frac{1}{v-z} \right. \\ &\quad \left. - \frac{1}{2} \mathcal{P} \int_1^\infty dz \frac{1}{\sqrt{z^2 - 1}} \frac{1}{v-z} \right\}, \end{aligned} \quad (\text{C.20})$$

$$\begin{aligned} \text{Re } \Pi_{-+}(k, \omega) &= \frac{1}{\pi\gamma^2} \frac{\gamma k}{4} \left\{ n\Lambda^2 \frac{I_1(u)}{u} \mathcal{P} \int_1^\infty dz \frac{e^{-uz}}{\sqrt{z^2 - 1}} \frac{1}{v+z} \right. \\ &\quad \left. - \frac{1}{2} \mathcal{P} \int_1^\infty dz \frac{1}{\sqrt{z^2 - 1}} \frac{1}{v+z} \right\}. \end{aligned} \quad (\text{C.21})$$

Combining intraband and interband contributions, respectively, we obtain

$$\begin{aligned} \text{Re } \Pi_{\text{intra}}(k, \omega) &= \text{Re } \Pi_{++}(k, \omega) + \text{Re } \Pi_{--}(k, \omega) \\ &= -\frac{n\Lambda^2}{\pi^2\gamma^2} \frac{\gamma k}{4} \frac{K_1(u)}{u} \mathcal{P} \int_{-1}^1 dt \frac{e^{ut} - e^{-ut}}{\sqrt{1-t^2}} \frac{1}{t-v} \\ &= -\frac{n\Lambda^2}{\pi^2\gamma^2} \frac{\gamma k}{4} \frac{K_1(u)}{u} \mathcal{R}(u, v), \end{aligned} \quad (\text{C.22})$$

$$\begin{aligned} \text{Re } \Pi_{\text{inter}}(k, \omega) &= \text{Re } \Pi_{+-}(k, \omega) + \text{Re } \Pi_{-+}(k, \omega) \\ &= -\frac{1}{\pi\gamma^2} \frac{\gamma k}{4} \left\{ n\Lambda^2 \frac{I_1(u)}{u} \mathcal{P} \int_1^\infty dz \right. \\ &\quad \times \frac{e^{-uz}}{\sqrt{z^2 - 1}} \left[\frac{1}{v-z} - \frac{1}{v+z} \right] \\ &\quad \left. - \frac{1}{2} \mathcal{P} \int_1^\infty dz \frac{1}{\sqrt{z^2 - 1}} \left[\frac{1}{v-z} - \frac{1}{v+z} \right] \right\} \\ &= -\frac{1}{\pi\gamma^2} \frac{\gamma k}{4} \left\{ n\Lambda^2 \frac{I_1(u)}{u} \mathcal{S}(u, v) \right. \\ &\quad \left. + \frac{\pi}{2} \frac{1}{\sqrt{1-v^2}} \Theta(1-v) \right\}. \end{aligned} \quad (\text{C.23})$$

The remaining integrals $\mathcal{R}(u, v)$ and $\mathcal{S}(u, v)$ in (C.22) and (C.23) are very interesting mathematical objects. To further analyze them, we convert $\mathcal{S}(u, v)$ into a similar shape as $\mathcal{R}(u, v)$ by substituting $t = 1/z$,

$$\mathcal{S}(u, v) = \frac{1}{v} \mathcal{P} \int_{-1}^1 dt \frac{e^{-\frac{u}{|t|}}}{\sqrt{1-t^2}} \frac{1}{t - \frac{1}{v}}. \quad (\text{C.24})$$

Resistant against all efforts to solve them analytically, $\mathcal{R}(u, v)$ and $\mathcal{S}(u, v)$ turn out to be equivalent to a certain kind of integral transformation between Chebyshev series of first and second kind. We use the following relation [32]:

$$\text{If } f(y) \sim \sum_{n=1}^{\infty} a_n T_n(y) \text{ and } g(x) \sim \pi \sum_{n=1}^{\infty} a_n U_{n-1}(x) \text{ then}$$

$$g(x) = \mathcal{P} \int_{-1}^1 dy \frac{f(y)}{\sqrt{1-y^2}(y-x)}, \quad (\text{C.25})$$

T_n and U_n are the Chebyshev polynomials of first and second kind, respectively [17]. Note that (C.25) holds only for $|x| \leq 1$.

Most importantly, the expansion coefficients of the series are the same on both sides. Therefore, if one knows the Chebyshev series (of first kind) of the numerator function, the series (of second kind) of the sought function is known, too.

In $\mathcal{R}(u, v)$, the numerator function is just the hyperbolic sine function. The coefficients of the Chebyshev series of first kind of $f(z, u) = \sinh uz$ are given by [32]

$$a_n^{(\mathcal{R})}(u) = \frac{2}{\pi} \int_{-1}^1 dz \sinh uz \frac{T_n(z)}{\sqrt{1-z^2}} = \begin{cases} 0 & \text{if } n = 2k \\ 2I_n(u) & \text{if } n = 2k+1, \end{cases} \quad (\text{C.26})$$

where I_n again denotes the modified Bessel function of first kind [17].

The relation (C.25) has to be modified for $|x| > 1$. In that case, $g(x)$ has to be complemented according to

$$g(x) \sim \pi \sum_{n=1}^{\infty} a_n \left[U_{n-1}(x) - \frac{T_n(x)}{\sqrt{x^2-1}} \right]. \quad (\text{C.27})$$

Therefore, one obtains for $\mathcal{R}(u, v)$ with (C.25)–(C.27):

$$\mathcal{R}(u, v) = 4\pi \sum_{k=0}^{\infty} I_{2k+1}(u) \{ U_{2k}(v) \Theta(1-v) \Theta(1+v) + \left[U_{2k}(v) - \frac{T_{2k+1}(v)}{\sqrt{v^2-1}} \right] \Theta(v-1) \Theta(-v-1) \}. \quad (\text{C.28})$$

In $\mathcal{S}(u, v)$, the numerator function is $e^{-\frac{u}{|z|}}$. The coefficients of the Chebyshev series of first kind have to be determined from

$$a_n^{(\mathcal{S})}(u) = \frac{2}{\pi} \int_{-1}^1 dz e^{-\frac{u}{|z|}} \frac{T_n(z)}{\sqrt{1-z^2}}, \quad (\text{C.29})$$

and $\mathcal{S}(u, v)$ is then given by

$$\mathcal{S}(u, v) = \frac{\pi}{v} \sum_{k=1}^{\infty} a_k^{(\mathcal{S})}(u) \{ U_{k-1}(1/v) \Theta(1-1/v) \Theta(1+1/v) + \left[U_{k-1}(1/v) - \frac{T_k(1/v)}{\sqrt{1/v^2-1}} \right] \times \Theta(1/v-1) \Theta(-1/v-1) \}. \quad (\text{C.30})$$

Summarizing all contributions to imaginary and real parts of the polarization function of a graphene-like two-

dimensional semiconductor structure, we have

$$\text{Im } \Pi(k, \omega) = \sum_{a,b} \text{Im } \Pi_{ab}(k, \omega)$$

$$= \frac{1}{\gamma^2} \frac{\gamma k}{4} \left\{ \frac{n\Lambda^2}{\pi} \frac{e^{-\frac{\beta\hbar\omega}{2}} - e^{\frac{\beta\hbar\omega}{2}}}{\sqrt{1-\left(\frac{\hbar\omega}{\gamma k}\right)^2}} \frac{K_1\left(\frac{\beta\gamma k}{2}\right)}{\beta\gamma k/2} \right.$$

$$\times \Theta\left(1 - \frac{\hbar\omega}{\gamma k}\right) \Theta\left(1 + \frac{\hbar\omega}{\gamma k}\right)$$

$$+ \left[n\Lambda^2 \frac{e^{-\frac{\beta\hbar\omega}{2}}}{\sqrt{\left(\frac{\hbar\omega}{\gamma k}\right)^2 - 1}} \frac{I_1\left(\frac{\beta\gamma k}{2}\right)}{\beta\gamma k/2} - \frac{1}{2} \frac{1}{\sqrt{\left(\frac{\hbar\omega}{\gamma k}\right)^2 - 1}} \right]$$

$$\times \left[\Theta\left(\frac{\hbar\omega}{\gamma k} - 1\right) - \Theta\left(-\frac{\hbar\omega}{\gamma k} - 1\right) \right] \}, \quad (\text{C.31})$$

$$\text{Re } \Pi(k, \omega) = \sum_{a,b} \text{Re } \Pi_{ab}(k, \omega)$$

$$= -\frac{1}{\gamma^2} \frac{\gamma k}{4} \left\{ \frac{n\Lambda^2}{\pi^2} \frac{K_1\left(\frac{\beta\gamma k}{2}\right)}{\beta\gamma k/2} \mathcal{R}\left(\frac{\beta\gamma k}{2}, \frac{\hbar\omega}{\gamma k}\right) \right.$$

$$+ \frac{n\Lambda^2}{4\pi} \frac{I_1\left(\frac{\beta\gamma k}{2}\right)}{\beta\gamma k/2} \frac{\gamma k}{\hbar\omega} \mathcal{S}\left(\frac{\beta\gamma k}{2}, \frac{\gamma k}{\hbar\omega}\right)$$

$$\left. + \frac{1}{2\sqrt{1-\left(\frac{\hbar\omega}{\gamma k}\right)^2}} \Theta\left(1 - \frac{\hbar\omega}{\gamma k}\right) \Theta\left(1 + \frac{\hbar\omega}{\gamma k}\right) \right\}, \quad (\text{C.32})$$

where $\mathcal{R}(u, v)$ and $\mathcal{S}(u, v)$ are given by (C.28) and (C.30).

Imaginary and real parts of the polarization function are depicted in figure C1 in the form

$$\Pi(k, \omega) = \frac{1}{4\beta\gamma^2} [\pi_1(k, \omega) + i\pi_2(k, \omega)] \quad (\text{C.33})$$

for a temperature of $1/\beta = 0.5R_X$ and different frequencies ω and degrees of quantum degeneracy $\chi = n\Lambda^2/2$. Note that, in this representation, π_1 and π_2 are independent on the specific material, its properties enter only via the excitonic Rydberg energy R_X and the overall prefactors.

The quantities exhibit the well-known principal behavior of Π for graphene-like systems (see, e.g., [23–26]), see left column in figure C1. The actual form of the curves, however, varies sensitively with the degree of quantum degeneracy. In the limiting case of vanishing degeneracy (equivalent to vanishing occupation of the upper cone), the remaining contributions (only from interband transitions) in (C.31) and (C.32) agree with the $\mu = 0$ ground state case derived, e.g., in [23, 26]. The corrections proportional to the degree of degeneracy modify the spectral structures both inside ($|\hbar\omega| > \gamma k$) and outside the cones ($|\hbar\omega| < \gamma k$) considerably as shown in the right column of figure C1.

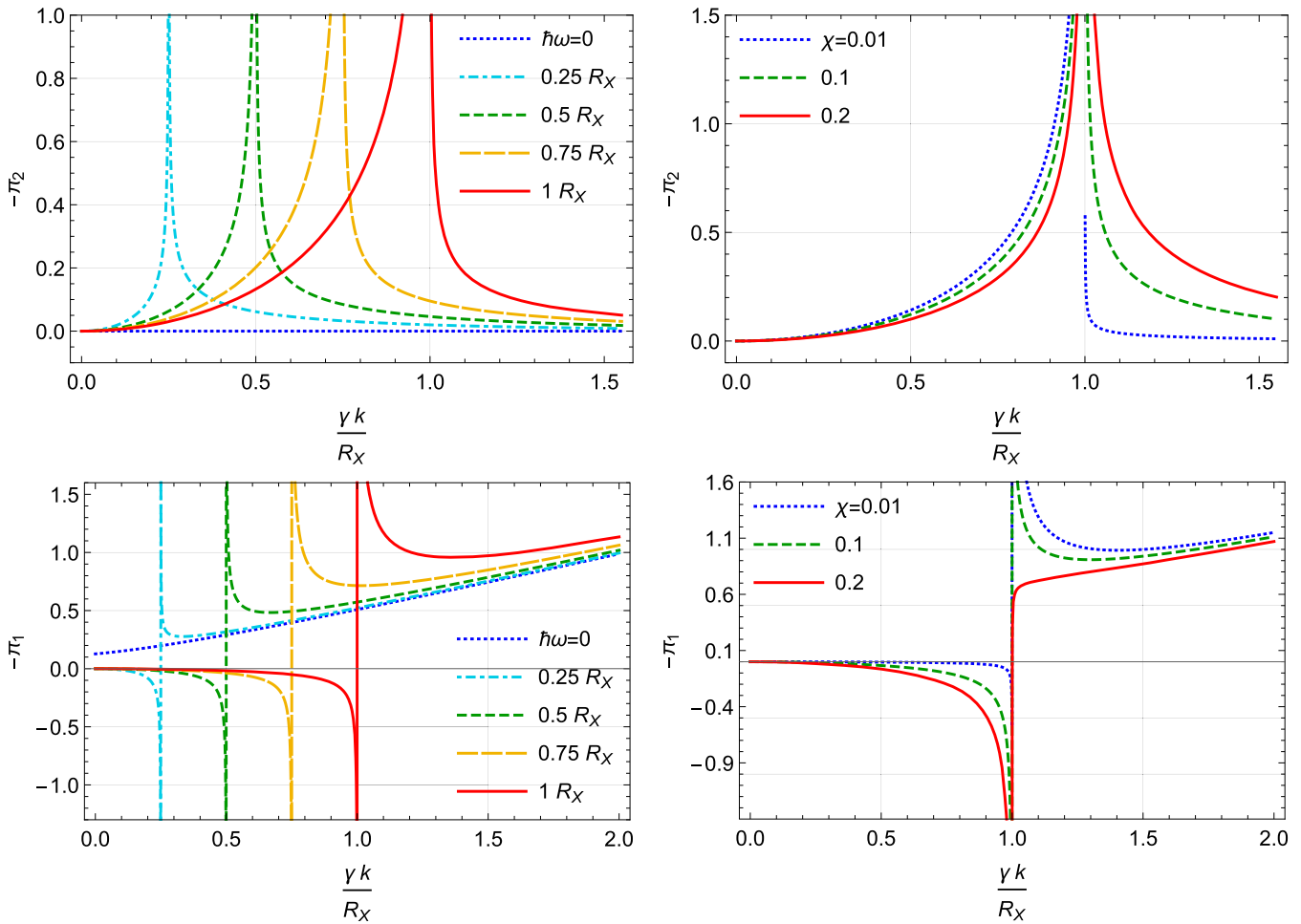


Figure C1. Imaginary (upper row) and real parts (lower row) of the polarization function for a two-dimensional system with linear carrier dispersion vs $\gamma k/R_X$ for a quantum degeneracy of $\chi = 0.05$ and several $\hbar\omega$ (left panels) and for $\hbar\omega = 1R_X$ and several χ .

ORCID iDs

D Semkat <https://orcid.org/0000-0002-2179-9064>

H Stolz <https://orcid.org/0000-0002-2678-3854>

References

- [1] Mahan G 2000 *Many Particle Physics* 3rd edn (New York: Plenum)
- [2] Kraeft W D, Kremp D, Ebeling W and Röpke G 1986 *Quantum Statistics of Charged Particle Systems* (New York: Plenum)
- [3] Kremp D, Schlanges M and Kraeft W-D 2005 *Quantum Statistics of Nonideal Plasmas* (Berlin: Springer)
- [4] Arndt S, Kraeft W D and Seidel J 1996 *Phys. Status Solidi b* **194** 601
- [5] Kazimierczuk T, Fröhlich D, Scheel S, Stolz H and Bayer M 2014 *Nature* **514** 343
- [6] Heckötter J et al 2018 *Phys. Rev. Lett.* **121** 097401
- [7] Versteegh M A M et al 2021 arXiv:2105.07942v1
- [8] Semkat D, Fehske H and Stolz H 2019 *Phys. Rev. B* **100** 155204
- [9] Semkat D, Fehske H and Stolz H 2021 *Eur. Phys. J. Spec. Top.* **230** 947
- [10] Raja A et al 2017 *Nat. Commun.* **8** 15251
- [11] Castro Neto A H, Guinea F, Peres N M R, Novoselov K S and Geim A K 2009 *Rev. Mod. Phys.* **81** 109
- [12] Hasan M Z and Kane C L 2010 *Rev. Mod. Phys.* **82** 3045
- [13] This includes models where the self-energy is approximated by a momentum-independent quantity (*rigid shift*) since such contributions cancel each other in the difference.
- [14] Fehr R and Kraeft W-D 1994 *Phys. Rev. E* **50** 463
- [15] Seidel J, Arndt S and Kraeft W D 1995 *Phys. Rev. E* **52** 5387
- [16] Klimontovich Yu L and Kraeft W D 1974 *Teplofiz. Vys. Temp.* **12** 239
Klimontovich Yu L and Kraeft W D 1975 *High Temp. (USSR)* **12** 212 (Engl. Transl.)
- [17] Abramowitz M and Stegun I A 1965 *Handbook of Mathematical Functions: With Formulas, Graphs, and Mathematical Tables (Dover Books on Advanced Mathematics)* ed M Abramowitz and I A Stegun (New York: Dover)
- [18] Rytova N S 1965 *Dokl. Akad. Nauk SSSR* **163** 1118
Rytova N S 1967 *Vestn. Mosk. Univ.* **3** 30
- [19] Keldysh L V 1979 *Pis'ma Zh. Eksp. Teor. Fiz.* **29** 716
Keldysh L V 1979 *JETP Lett.* **29** 658 (Engl. Transl.)
- [20] Selig M 2018 Exciton-phonon coupling in monolayers of transition metal dichalcogenides *PhD Thesis* TU Berlin
- [21] Girndt A, Jahnke F, Knorr A, Koch S W and Chow W W 1997 *Phys. Status Solidi b* **202** 725
- [22] Mancke G, Semkat D and Stolz H 2012 *New J. Phys.* **14** 095002
- [23] Shung K W-K 1986 *Phys. Rev. B* **34** 979
- [24] Hwang E H and Das Sarma S 2007 *Phys. Rev. B* **75** 205418
- [25] Kotov V N, Uchoa B, Pereira V M, Guinea F and Castro Neto A H 2012 *Rev. Mod. Phys.* **84** 1067

- [26] Wunsch B, Stauber T, Sols F and Guinea F 2006 *New J. Phys.* **8** 318
- [27] Stolz H et al 2012 *New J. Phys.* **14** 105007
- [28] Bastard G 1988 *Wave Mechanics Applied to Semiconductor Heterostructures* (Paris: Les Editions de Physique)
- [29] Fox M and Ispasoiu R 2006 *Quantum Wells, Superlattices, and Band-Gap Engineering (Springer Handbook of Electronic and Photonic Materials)* ed S Kasap and P Capper (Berlin: Springer) pp 1021–40
- [30] <http://ioffe.ru/SVA/NSM/Semicond/AlGaAs/basic.html>
- [31] Belov P A 2019 *Physica E* **112** 96
- [32] Mason J C and Handscomb D C 2003 *Chebyshev Polynomials* (London: Chapman and Hall)